20

Crystallization, Fractionation and Solidification of Co-Magmatic Alkaline Series Sequentially Emplaced in the Carbonatite Complex of Tiruppattur, Tamil Nadu, India

R. Ramasamy
Ocean Engineering, IITM, Chennai, India

1. Introduction

A mineral is naturally occurring substance with a characteristic crystal structure and chemical composition. It occurs in rocks. Frequently, it has homogeneous crystalline structure in which one or more types of atoms or molecules may be partially substituted for the original atoms and molecules without changing the structure. Thus, most rock-forming minerals are formed in solid solutions. Aggregates of minerals produce characteristic rock-textures which shed light on their trends of magmatic evolution. They crystallize from molten rock, called magma. Magmas are a natural material of hot silicate / carbonate /oxide / phosphate/ sulphide and sulphur melts from which igneous rocks form. They develop by the partial melting of deep-seated rocks at depth. Primary melts are composed of suspended crystals and dissolved gases. The crystallization of a primary melt and the isolation of the rest liquid freed from suspended solids are called the parent magma, which then produces a series of residual magmas of a secondary nature with varying compositions through differentiation and fractionation. The molten material is necessarily forced to the surface, either by hydrostatic head in the mantle where the encasing rock is denser than the melt or else via gas by propulsion. Pressure enhances the solubility of H_2O and other volatiles, which lower the equilibrium temperature of solidification. These volatile substances may largely escape during the course of the ascension of the magma as well as during the course of crystallization. Rising toward the Earth's surface, the magma enters zones of lower temperatures and pressures. Decreasing temperatures tend to bring about crystallization, which produces solid crystals suspended in the liquid. Other solid fragments are incorporated from the walls and roof of the conduit through which the magma is rising and the magma changes its composition by assimilation. A closed magmatic chamber is formed by the filling up of magma in cavities at intermittent stopping places. Over the course of the magmatic crystallization of the parent magma in a closed magmatic chamber, volatiles may be concentrated and interacted with minerals during slow cooling. Magma is generally composed of eight major oxides SiO_2, Al_2O_3, Fe_2O_3, FeO, MgO, CaO, Na_2O and K_2O, as well as from lesser proportions of TiO_2, P_2O_5, H_2O, CO_2, S and other volatiles. In addition to these there are other substances constituting various gases and trace elements. As crystallization progresses, the volatiles and the more soluble silicate components are concentrated in the

remaining liquid. They increase the fluidity of the magma. Moreover, they do not enter appreciably into the earlier minerals forming from the magma, but are instead finally concentrated in an aqueous solution as hydrothermal fluid. Minerals initially crystallized from the magma are denser than the magma and buoyancy forces lead to gravity settling the crystals. In some rare and denser iron-rich or carbonatite magmas, feldspar crystals may float. The viscosity of silicate magma generally increases with a decrease in the temperature - with decreases in dissolved H_2O - with an increase in crystal fraction and an increase in the degree of SiO_2 content.

2. Polymerization

The polymerization of silicate melt takes place by the reaction of a silicate melt to form three dimensional networks of SiO_4 chains. This structure of a silicate melt provides information on its structure and physical, chemical and thermal properties. From this information, it is possible to understand the conditions of crystallization and the evolution of the silicate minerals from the melt /magma. In magmatic processes, phase equilibria in melt-crystal-vapour systems, diffusion in melts and the thermodynamic, electrical and rheological properties of magma systems are of particular importance. Silicate minerals essentially contain silicon and oxygen in the form of a network of tetrahedra in which a Si ion is surrounded by 4 oxygen ions. The tetrahedra occur as isolated $(SiO_4)^{4-}$ or else joined together in various ways, such as $(Si_2O_7)^{6-}$ and rings $(Si_6O_{18})^{12-}$. Ortho-silicates have isolated $(SiO_4)^{4-}$ tetrahedra that are connected only by interstitial cations. Sorosilicates have isolated double tetrahedral groups with $(Si_2O_7)^{8-}$. Cyclosilicates have linked tetrahedra with $(Si_xO_{3x})^{2x-}$. Inosilicates have interlocking chains of silicate tetrahedra with either SiO_3 for single chains or Si_4O_{11} for double chains. Sheet-silicates form parallel sheets of silicate tetrahedra with Si_2O_5. Tectosilicates have a three-dimensional framework of silicate tetrahedra with SiO_2. As a silicate melt cools, minerals crystallize that are in equilibrium with the melt. Ortho-silicates like olivine generally crystallize from a silicate melt at a very high temperature in a disordered state; on the other hand, quartz and alkali feldspar crystallize from the melt at a relatively low temperature state. At the ends of the scale, the structural states of silicate melts vary widely. Similarly, within the crystallizing minerals, the olivine crystallizing at the early stage of magmatic evolution and the quartz crystallizing at very high temperature states at the late magmatic stage are deficient in Si ions in their tetrahedral co-ordinations. Thus, the structural states of co-existing minerals and the silicate melt from which they crystallize vary widely. In studying such variations, it is possible to see the trend of magmatic evolution. Magmatic evolution may reveal the cooling history of minerals and their accompanying rocks. Volcanic rock which has been suddenly quenched also reveals genetic relationships between phenocrysts and their groundmass matrix, which represents a quenched silicatemelt. There exists a genetic relationship between the structure of a silicate melt and the structure of the silicate mineral crystallizing stemming from it. For example, under an increase of alkalis and alkaline earth elements in the silicate melt, tetrahedrally co-ordinated Al^{3+} displays a strong preference for three-dimensional network units in the form of feldspars in the silicate melts with an increase of the Al/(Al+Si) of the melt and a decrease of SiO_4^{4-} units in the melt (Mysen et al., 1985). The structure of a silicate melt depends upon the viscosity of the melt and the subsolidus structure of the crystallizing silicate mineral at a high temperature state. Under these favourable conditions, the crystal-melt equilibrium of the partition of one element between them sets. Magmatic evolution can be traced by studying the changes of the structural state of crystallizing minerals and the

changes in structure of residual melts in spatial and temporal conditions. Slow cooling permits extensive large crystal growth under plutonic magmatic crystallization. As melting and crystallization are reversible processes, different types of phase diagrams are needed to understand how melts crystallize. Magmatic liquids have a sub-solidus structure which is created largely by varying the degrees of bonding among SiO_4 tetrahedra (polymerization). The difference between a silicate liquid and a silicate mineral is that the mineral has a definite long-range order structure that is the same throughout while a silicate melt shows different types of the short-range order of polymerization throughout the melt. Additionally, the degree of the polymerization of the melt controls the viscosity of the melt. Mafic magmas that have relatively low Si contents have depolymerized melts that produce depolymerized crystals - like olivine or pyroxene - and these melts tend to have a high temperature and a low viscosity. In contrast, felsic magmas have abundant Si and Al, whereby the melts are highly polymerized owing to their high viscosity such that they crystallize as sheet and framework silicates. Because of these consequences, Mg-Fe-rich basaltic magmas erupt easily and the lavas flow several kilometres from their vents, while the Si-rich rhyolite lava erupts explosively without escaping out of its inherent gas bubbles. Volatiles are elements that dissolve in magmas but transform to gas when magma crystallizes or because of a sudden decrease in pressure. The eolution of magmatic rocks may be traced out based on the concept of "Bowen's Reaction Series". The order of crystallization of common plagioclase feldspars from cooling magma is evolved from Ca-rich to more Na-rich plagioclase feldspars as a continuous series during decreasing temperature. The high temperature olivine would react with residual magma and change to the next mineral pyroxene in the series. Pyroxene continues to cooling, it would convert to amphibole and then biotite by adjusting the mineral crystalline lattice to achieve stability of different temperatures as discrete minerals. At lower temperatures both continuous and discrete series merge together and orthoclase, muscovite and quartz tend to crystallize. The difference in crystallization temperatures for different kinds of minerals plays a major role in the differentiation of rock composition as magma cools. Thus, various types of magmatic rocks from the early formed ultamafic peridotites to granitic rocks at the late magmatic stages are evolved (Bowen, 1956). Bowen's reaction series show that one homogeneous body of magma can form more than one kind of igneous rock. It reveals the relationship between cooling magma and the formation of minerals that make up igneous rocks.

Some generalizations:

1. The compositional paths followed by both the melts and the growing crystal depend on the initial bulk composition of the melt.
2. The composition of both the melt and the crystal at any point in the crystallization process is dependent on the extent to which the crystallization process has been completed.
3. For minerals that exhibit a solid solution, crystallization proceeds in a continuous manner with the composition of the mineral changing along with that of the magmatic liquid.
4. For minerals that do not exhibit a solid solution, melting or crystallization will proceed in discrete discontinuous steps. As a melt cools, such discrete minerals will appear suddenly when the melt reaches the appropriate temperature.
5. Minerals that crystallize at high temperatures are rich in Mg and Fe and relatively poor in Si.

6. Minerals that crystallize at the lowest temperatures are rich in Si and Al.
7. Intermediate minerals that crystallize at intermediate temperatures are intermediate in relation to Si.
8. Another important observation in that those minerals which crystallize at high temperatures show less polymerization of the Si-tetrahedra than those which crystallize at lower temperatures.
9. The discrete mineral sequences starts with orthosilicates (olivine), single chain (pyroxene), double chain (amphibole) and sheet silicates (biotite), and exhibit a high degree of silica polymerization with incorporations of H_2O, F and other volatiles. The crystallization of plagioclase in a continuous series also indicates an increase of silica constituents, even though they crystallize in framework silicates.
10. Highly polymerized silica-rich tectosilicates are more stable than silica-poor tectosilicates. The degree of polymerization increases from orthosilicates to tectosilicates.
11. The initial crystallization of olivine, the residual magma, is enriched in silica.
12. The initial crystallization of pyroxene under dry conditions, the residual liquid, is deficient silica.
13. The initial crystallization of alkali pyroxene, alkali amphibole, biotite or magnetite, from a silica undersaturated volatile-rich basic alkali magma, residual magma slowly gets enriched with silica and finally at the late magmatic stages free quartz crystallizes in significant amount as an end product.
14. Rock textures are controlled by conditions of crystallization and cooling. Studying rock textures and the mode of the occurrence of rock types in the field, it is possible to correlate rocks and minerals.

The most common magma which is rich in silica is highly polymerized and has a low activity of oxygen ions and a basic magma rich in MgO and CaO has a high activity of oxygen ions. During the course of crystallization, the most abundant, least soluble mineral grows first followed by the less abundant, more soluble substances from the magma. During the course of crystallization, silicate magma displays progressive enrichments of both soda relative to lime and ferrous iron relative to magnesia in crystals and residual melts. Slowly ascending very hot magmas may cool before reaching the surface.

The crystallization of minerals from magma is a complex process because of changes in the temperature, pressure and composition (TPX). The TPX can have dramatic effects on the order of crystallization and the order-disorder structural state of various minerals in a sequence. The addition or loss of water, CO_2, H_2 and O_2 changes the course of magmatic differentiation. The initial crystallization and separation of early-formed minerals from the residual liquid plays a critical role in the trend of magmatic evolution. The general order of crystallization from the magma is as follows: a) low silica containing basic minerals, such as olivine and calcic plagioclase, together with non-silicate minerals, b) medium-silica-bearing minerals, such as clinopyroxene or labradorite, c) high silica-bearing minerals, such as orthoclase and quartz. Depending on the initial chemical composition of the common basaltic magma, either plagioclase or pyroxene may start to crystallize first, changing the composition of the residual magma until simultaneous crystallization occurs. Slight differences in the composition of the parent basaltic magma may result in the production of an end-magma which is either over-saturated or under-saturated in silica (Barth, 1962). The early crystallization and fractionation of olivine / plagioclase / diopside, the respective residual liquid, is progressively enriched in silica over-saturated rocks (Bowen, 1956) or else

alumina poor or silica under-saturated rocks (Barth, 1962) or silica under-saturated alkali-aluminium silicates (Schairer and Yoder, 1960). If the crystal's settling and fractionation are irregular, the composition of the residual magma continuously changes over the course of time. The early crystallized and fractionated silicate or non-silicate mineral from the magma controls the chemical composition of the residual melt and its subsequent trend of crystallization. The composition of the parent magma and its volatile constituents decide which of the minerals start the initial crystallization. Only by studying the field relationship, petrographic features and compositions of the minerals in the rocks and their mode of occurrence and geological setting, along with experimental results, is it possible to trace the magmatic evolution of co-magmatic series of rocks.

3. Magmatic melt structure

The kinetic properties of magma depend upon the atomic mobility within variably polymerized silicate melts. Most polymerized silicic crystal fractions affect the properties of melts by resisting shear deformations. They provide bases for polymerized links to attach in melts' rich fluids and by providing porous networks for the melts and the chemical species within them to flow or diffuse from one location to another. Crystals with large interfacial angles (>60 degrees) represent a near collapse of the grain-supported structure, which can act to either press out or lock melt fractions from one another within a crystal – a melt mush at lower temperatures. Therefore, it may also be impossible to initiate the types of grain boundary movements continuously needed for both minerals in new solutions. This may have an impact on grain compositions, resulting in the zoning of the crystals that form silicic melts becoming more viscous. The magmatic melt structure is viewed as linkages of Si^{4+} and Al^{3+} ions in tetrahedral coordination with O^{2-}ions. They are polymerized in the more Si-Al rich melts. Dissolved water breaks the Si-O chains and reduces the degree of polymerization and makes it less viscous. The presence of CO_2 rich fluid inclusions in calcites, feldspars, pyroxenes and olivines (Ramasamy and Shapenko, 1980) could be considered to be vapour trapped phases during the growth of these minerals. In addition to H_2O, the vapour phases of CO_2, SO_3, and P_2O_5 play a critical role in the viscosity of the melt.

The formation of crystal nucleus and crystal growth or the accretion of atoms onto the nucleus may take place in two or more stages, depending upon the kinetic conditions of the magma. Microlites are relatively associated with higher energies of surface tension and surface energies than their associated phenocrysts. The rates of growth increase with the increasing of under-cooling up to a maximum value and then diminish. High nuclei populations yield fine-grained rocks. The close associations of both fine-grained aplitic syenites and coarse-grained pegmatitic syenites with subvolcanic miarolitic crystallizations indicate wide variations in the textural pattern of the alkaline rocks in the area under study. The drastic cooling of highly viscous melts produces amorphous glass. Vitrophyric textures are produced by rapid cooling while emplacement occurs in some dolerites in this area. Complex minerals with solid solution relationships often grow when their growth rates are faster than their diffusion rates. The diffusion of chemical constituents is due to variations in the thermal energy in the magmatic chamber. Zoned plagioclases, clinopyroxenes, zoned alkaline rocks and zoned carbonatites are evolved in this manner. An increase of volatile proportions in late magmatic melts produces boiling, exsolution and / or vesiculation in the residual rocks. The sizes of comagmatic bodies and their volumes during fractionation in sequences and subsequent emplacements also play vital roles in evolution of melt structures at various levels of emplacements as well as in

residual magmas. In studying the order / disorder relationships and partitioning elements, it is possible to trace the cooling history of the magma.

4. Carbonatite complex

The carbonatite complex of Tiruppattur (12° 00′00″-12°30′00″N and 78°25′00″-78°35′00″E) Tamil Nadu India is an ideal area to trace magmatic evolution and its magmatic zonal variations (Fig. 1). It is unique in its geological settings, in the fractional crystallization of various minerals crystallized during the course of a prolonged period of magmatic differentiation, and in the emplacement of co-magmatic zoned alkaline rocks and the immiscible separation of carbonatites and alkali syenites from common parent magma. The geological field settings present in this area indicate the occurrences of co-magmatic sequences of both silica undersaturated series of rocks and silica oversaturated series of rocks together. Both these series of rocks have co-magmatic relationships and continuous compositional variations among mineral assemblages. Progressive enrichment of alkali, silica and volatile constituents plays a critical role during the course of magmatic evolution from a highly silica undersaturated shonkinite magma to silica oversaturated alkali syenite or granite magma under favourable tectonic environment..

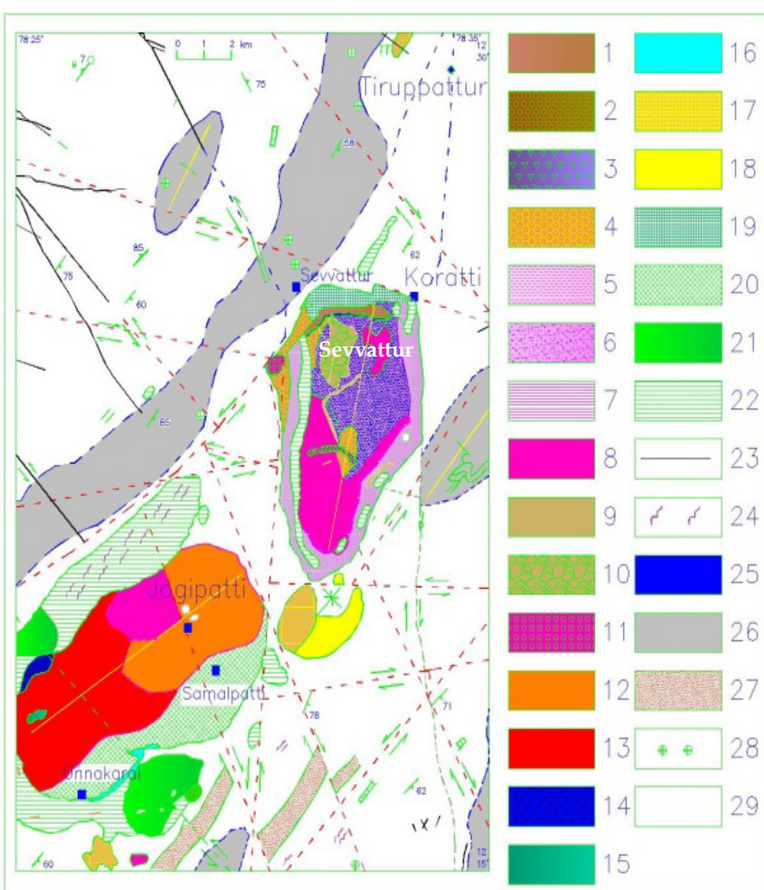

1. Carbonatite,
2. Shonkinite,
3. Vogesite,
4. Oligoclasite,
5. Hornblende syenite,
6. Hornblende porphyritic syenite,
7. Augite syenite,
8. Porphyritic augite syenite,
9. Foliated syenite,
10. Foliated porphyritic syenite
11. Hornblede biotite syenite,
12. Riebeckite syenite,
13. Garnetiferous syenite,
14. Microcline garnet syenite,
15. Wollastonite syenite,
16. Skarn,
17. Granite
18. Granodiorite,
19. Biotite oligoclase pyroxenite
20. Biotite pyroxenite,
21. Ultrabasics
22. Ultramafics,
23. Dolerite,
24. Pegmatite-aplite
25. Albitite
26. Charnockite,
27. Pyroxene granulite,
28. Norite,
29. Granite gneiss

Fig. 1. a. Geological map of the carbonatite complex of Tiruppattur, India

Fig. 1. b. Structural sketch map

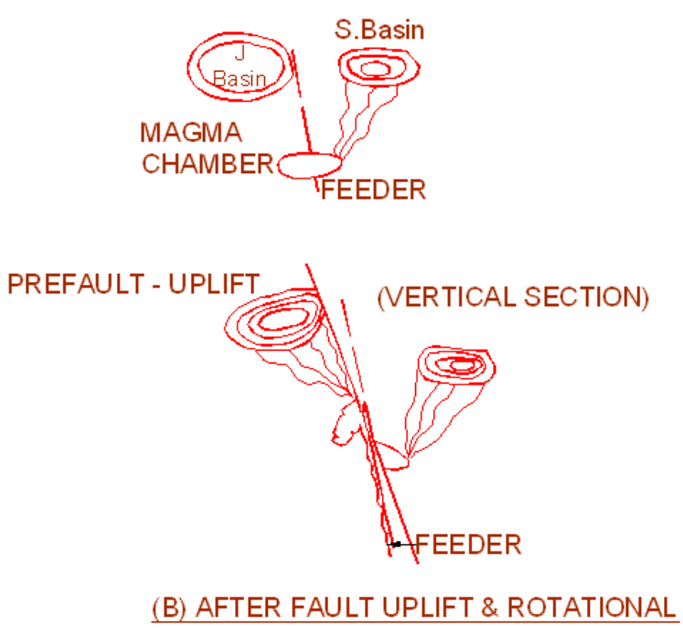

Fig. 1. c. Parent magma ascending from a deep-seated source filled in a magmatic chamber

5. Methodology

Several fieldtrips and observations were made during the course of geological mapping. Thin sections were prepared for various rocks collected in the field and studied under a universal stage (Naidu, 1958) attached polarizing microscope for the identification and determination of the volume proportions of the minerals.

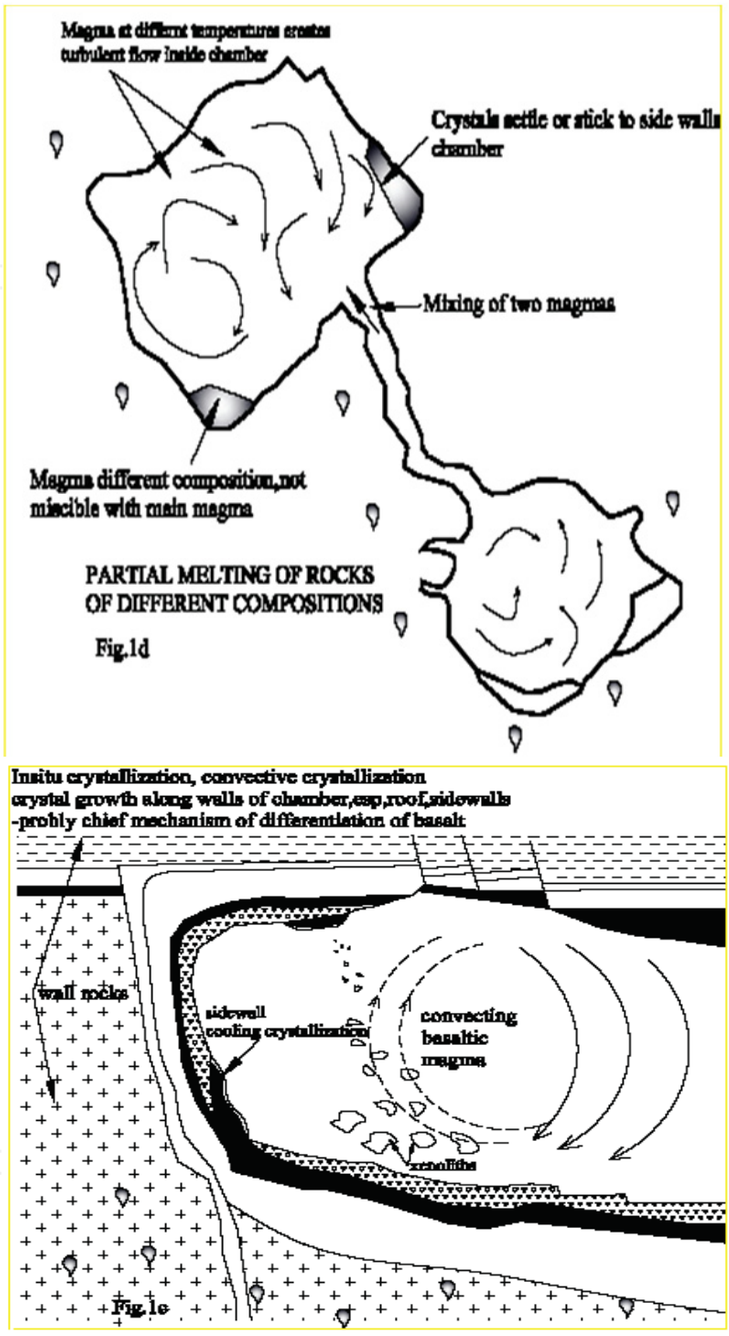

Fig. 1. d. The partial melting of rocks of different compositions concentrates in some large cavities of magmatic chambers. Hot magma rising from the feeder chamber mixes with the already existing magma at a relatively lower temperature and turbulently circulates inside the magmatic chamber. Some of early-formed crystals stick to the walls. The pre-existing magma may dissolve with the incoming magma and mixes with it. The undissolved immiscible magma of different compositions may settle at certain portions. Fig. 1e Magma ascending through fractures breaks the wall rock into pieces of rock fragments which are assimilated by the magma while the magma changes its composition.

i. Differentiation and fractionation of the parent magma for a quiescent prolonged period
ii. Emplacements of a series of soda-rich comagmatic syenites and carbonatites in the Sevvattur Basin
iii. Shifting of the magmatic emplacements of potash rich co-magmatic alkali series and carbonatites into the continuously uplifted and rotated Jogipatti Basin towards the SW
iv. The two basins are enclosed with ultrabasic rocks

By measuring the relationships between the crystallographic and optic axes of the chemical compositions of the minerals and their order-disorder, the structural features are estimated. The textural and structural features of the mineral assemblages, the order of crystallization of the crystallization of the minerals and their magmatic evolutions are traced. The composition of feldspar grains, Fe-Mg ratios in olivine, pyroxene, amphiboles and biotite were calculated by measuring the refractive indices and by finding the optical properties and using the appropriate nomograms given in the texts (Winchell, 1945; Deer et al., 1965). X-ray powder diffraction analyses were made to study the order-disorder relationship by measuring the triclinicity of the feldspars and the M2, M1 and T sites in the clinopyroxenes and the M_4 sites in the amphiboles. Staining techniques were adopted to distinguish calcite and ferro carbonates from dolomite, both in the laboratory as well as in the field (Dickinson, 1965). The chemical compositions of rocks were given by the conventional gravimetric analyses (author in the Geology Dept. Presidency College Chennai and Petrochemical Laboratory, Geology Faculty, Moscow State University) XRF and EDAX under a high resolution scanning electron microscope (IITM, Chennai) . The trace elements contents were determined by Atomic Absorption Spectrometry, Quartz –Grating Spectrograph and HR EDAX. These instrumental facilities were availed by the Department of Geology, Presidency College, Chennai, the Petrography Department, Faculty of Geology, Moscow State University, Russia, the Petrology laboratory, Department of Geology, Government of Tamil Nadu, Chennai and the Material Science Laboratory, Indian Institute of Technology Madras, Chennai.

6. Structure

The carbonatite complex is located in Tamil Nadu, India in a NE-SW trending rift valley formed between the Javadi Hills and the Elagiri Hills (Fig. 1 b), which are located within 5 km of one another. According to Grady (1971), the rift valley, bounded by fault planes, belongs to the category of the deep main faults of Peninsular India, extending more than 200 km in distance. Before rifting, the region was folded, faulted and uplifted by major tectonic deformations, trending with fold-axial plunges in the NW, N, NE, ENE, E and ESE directions. Owing to the number of re-worked fault systems occurring, since the Archaeans, the area has been dissected into several segments of block faults with rotational movements. Hence, it is very hard to analyse the age relationships of different fold styles. However, the regional pattern of fault systems present is seen around the carbonatite complex of Tiruppattur. The culmination of a NE-SW fold system caused the coeval and collinear formation of the Sevvattur and Jogipatti basins by the refolding of ultramafic, basic granulite, charnockite and granite gneiss (Fig. 1b & 1c). The regional NE-SW and N-S fault systems caused formation of a graben structure (Grady, 1971). Due to block faulting, the Jogipatti block was moved towards the west and then towards the north. The melting of the mantle rocks occurred at depth due to E-W crustal shear, which later provides an access route for the rising magma from a mantle source with intermittent stopping in a cavity, forming a closed magmatic chamber at depth. After a prolonged period of magmatic crystallization, differentiation and fractionation with the immiscible separation of

carbonatite magmas, the sequences of magmatic rocks were emplaced, first, in the Sevvattur basin and the block was then down warped. A forceful southern movement of the Sevvattur block abutting over the Jogipatti block caused an uplift and a rotational effect over which the rotational axis remained normal to the fault plane trending E-W and resting on the NE-SW fault plane. By the geometrical analysis of this fault system (Ramasamy, 1982), it was estimated that the Jogipatti basin was uplifted by more than 1000 m and, apparently, rotated by about 16° towards the east, and that it caused the emplacements of continuous sequences of late co-magmatic rocks. The magmatic activities were shifted to the latter basin from the original feeding source at depth (Fig. 1 b and 1 c). The generalized features of the magmatic activities are described in Fig. 1 d and 1 e.

7. Field relationship, mineralogical and textural variations in the alkaline complex

The carbonatite complex of Tiruppattur (Borodin et al., 1971; Saravanan and Ramasamy, 1971; Ramasamy, 1982) belongs to the Proterozoic Period, being around 800 Ma old (Schieicher et al., 1998). It is emplaced in two adjacent structural basins amidst Pre-Cambrian granite gneisses and charnockites (Fig. 1). Both of the basins are bounded by ultramafic rocks. The outer shell of the northern Sevvattur body is composed of a fine-grained speckled hornblende syenite with chilled margins and sharp contact with ultramafics and granite gneisses. Towards the south, the specked hornblende syenite imperceptibly grades into mottled augite syenite. The syenite complex exceeds 30 km^2 in extent. These syenites imperceptibly grade inwards towards the centre into their porphyritic syenite variants. The mottled porphyritic syenite is composed of large plates of feldspars containing smaller grains of feldspars in a matrix with accessories of aegirine augite, ferro-hastingsite, hornblende and magnetite. Large plates of plagioclase exhibit normal zoning from andesine to sodic oligoclase. The anorthite contents of the plagioclases decrease from the portions from the north to the south and from the peripheral portions towards the centre. The normal zoning and twinning of the plagioclase lamellae can be clearly seen in large platelets, even in hand-specimens. These rocks are essentially composed of alkali feldspars measuring up to 10 cm x 7 cm x 1 cm. The accessory mafic minerals are diopside, hornblende, augite and ferro-hastingsite. Feldspathic phenocrysts are present in the primary foliation of the rock. However, those mafic minerals occurring in the south are slightly coarse-grained, subhedral to euhedral in form, and are characteristically enriched in alkali constituents and potash feldspars. In places, cumulate feldspar phenocrysts with primary flow orientations are seen in some syenite bodies. The plagioclase and potash feldspars are composed of inclusions of plagioclases with complex twinning lamellae belonging to two or three generations and oriented in different directions. Microcline micro-perthite is commonly present in mottled porphyritic syenite. Albite lamellae, as blebs, orient along crystallographic directions. The plagioclase laths are increasingly plate-like and inform towards the centre of the basin. Similarly, the sizes of the mafic minerals increase and their compositions change with increases in alkali and ferric iron contents. Some places among the syenites - owing to the concentration of mafic minerals in felsic rocks or else the mush of feldspar phenocrysts in hypo-melanocratic syenites - form cumulate textures. The flow textures of feldspar phenocrysts and amphiboles are common in most of the syenites and they orient in the same directions. The rocks of the inner portions are successively younger than the rocks of the peripheral portions. The core portions are occupied by highly differentiated magmatic layers derived from deeper levels. Small veins of fine-grained

acmite-syenite are composed by a significant amount of magnetite and quartz and large plates of acmite are surrounded by the released products of magnetites. Abrupt variations from a porphyritic syenite to a non-porphyritic syenite are also seen. The impregnation of cumulates of feldspar phenocrysts into a syenite body is also seen. Many melanocratic streaks, thin slivers and patches of pyroxenites, are strewn as disseminated or as scattered material in the syenite body as mafic cumulates. The dissemination of mafic minerals is often crowded around mafic xenoliths. It seems to be the case that melanocratic rocks rich in mafic minerals are developed in this manner. Foliated fine-grained syenite occurs as a linear band in the porphyritic syenites in the Sevvattur basin. It exhibits crude foliation by the presence of abundant mica. In thin sections, it displays a xenomorphic granular texture. It is composed of oligoclase, anorthoclase, microcline, biotite, margarite and calcite. The grain size of the feldspar ranges from 0.1 mm to 0.3 mm. Discrete grains of microcline are formed as an interstitial to biotite. The replacement of oligoclase by potash feldspar is found along the cleavage planes. The development of patchy perthite is obvious: it imperceptibly grades into a pink coloured porphyritic syenite with a trachitoid texture. It occurs as a pale pink coloured rock with large plates of potash feldspar and oligoclase set in a fine-grained feldspathic matrix. Most of the feldspar platelets are square shaped with up to 5 cm sides. The breadth of the plates varies between 2 mm to 4 mm. In thin sections, feldspar displays an inequigranular poikilitic texture. Hornblende needles are present as inclusions within the plates of the feldspars and the needles orient in parallel towards the foliation planes of the rock. It is essentially composed of microcline, oligoclase and orthoclase, with accessories of chlorite, biotite, hornblende and epidote. The microcline and oligoclase are formed in two generations. Often, the feldspars are unoriented. They carry inclusions of fine needles of mafic minerals (with a helicitic texture) and show characteristic foliation. The core portion of the Sevvattur syenite body is occupied by oligoclasiteand albitite. The amphibole in the biotite-oligoclasite is altered into epidote granules and the amphibole is impregnated with felsic minerals producing a sieve texture. In some oligoclasites oligoclase and biotite, flakes exhibit a sheath texture with radiating platelets orienting towards a common centre. Along the peripheral portion of the carbonatite, albitite is exposed. In the albitite, the feldspar plates have inclusions of magnetite. The modal composition of potash feldspars varies widely and their content increases towards the core of the basin. Again, the volume percentage of the potash feldspars increases towards the south. Albitite, oligoclasite and biotite-bearing oligoclasites occur adjacent to the carbonatite body. A fine-grained monomineralic rock composed of more than 90% of albite in volume with accessories of magnetite and others exhibits the hypidiomorphic granular texture. Post magmatic growth of lueshite (sodium pyrochlore) in this rock produces expansion cracks in the surrounding albite. .

Syenite pegmatites and aplites are common in the carbonatite complex. They also occur as sheets along the fracture planes present in the syenites. Numerous anastomosing veins of pegmatites and aplites are seen in the syenites. Small bodies of pegmatites and aplites carry coarse-grained crystals along their borders. The mafic minerals grow towards it as shooting grains from the wall rocks and the core is only composed of felsic minerals. Massive bodies of pegmatites and aplites occupy over 50 km^2 in the Jogipatti basin. The northern portion of the syenite complex of this basin is composed of riebeckite-anorthoclase syenite while its southern portion is composed of orthoclase-bearing garnetiferous pegmatitic syenite. Garnetiferous syenite exhibits a hypidiomorphic granular texture. Euhedral to subhedral grains of garnets are embedded in the potash feldspar. The grossularite-andradite garnet gradually transforms into melanite towards the southwest of this region. Melanite-

microcline syenite, wollastonite syenite, wollastonite-scapolite syenite and wollastonite-melanite carbonatite are some of the aplitic veins found in this complex. Fine-grained microcline melanite syenite displays a xenomorphic granular texture. Micro-grains of microcline are surrounded by accessories of anhedral albite and melanite. These microclines and anorthoclases are highly disordered feldspars, having significant trace amounts of ferric iron. The biotite-syenite has a xenomorphic granular texture with euhedral to subhedral biotite. The biotite syenite porphyry is composed of large phenocrysts of anorthoclase, displaying zonal variation from the core to the periphery and set in a micro-granular feldspathic matrix. Such syenite porphyries are also composed of potash feldspar phenocrysts with a cryptoperthitic texture at the core and with homogeneous peripheral portions. The feldspars belong to two or more generations and they occur as large plates of phenocrysts as well as very small anhedral grains in the matrix. Younger aplites trend in N85^{o} crosscuts while older aplites trend in the N45^{o} direction. Small pockets of zircon- and magnetite-bearing syenites are seen in this basin. The miarolitic texture is a commonly seen in riebeckite pegmatites and aplites. This texture is produced by a crystal growth mechanism that was initially governed under the influence of surface-controlled kinetics. Larger crystals tend to grow by absorbing the required amount of water from the pore fluids present in the surrounding fine-grained matrix. Therefore, the fine-grained grains in the matrix are unable to grow larger due to a lack of water. Moreover, owing to their rapid cooling, larger phenocrysts formed at high temperatures exhibit lognormal rates of growth and in sizes relative to the small grains present in the matrix, forming syenite porphyries or porphyritic rocks under sub-volcanic conditions. The sudden increase of the viscosity of the residual magma also plays a critical role in the crystallization process of felsic and mafic minerals of two or more generations. Large crystals enclosing inclusions of euhedral feldspars oriented in two or three different directions are seen in mottled augite porphyritic syenite and this feature indicates slow cooling of the syenite magma followed by rapid ascending and consolidation of the magma. On the other hand, the anorthoclase-bearing miarolitic syenitic aplites and pegmatites carry abundant miarolitic cavities in which radiating needles of riebeckite are grown towards the centre of the cavities. Cross-cutting anorthoclase-bearing aplites are seen in mottled porphyritic syenites. Two generations of magnetite, apatite and zircon crystallize, both as early-formed minerals as well as very late-formed minerals. The late-formed minerals tend to have comparatively high ratios of surface area to volume. The large feldspar phenocryst platelets increasingly thin in speckled and mottled porphyritic syenites. Moreover, feldspars which crystallize very late in the mottled porphyritic syenite appear to be formed as early crystallized mineral in some of the agpaitic syenite pegmatites and aplites in the Jogipatti basin. The concentration of garnet, aegirine-augite or magnetite along a particular zone produces a banded structure. Radiating bundles and prisms of dark green riebeckite are seen in the aplitic riebeckite syenite and in the carbonatites of Jogipatti. All these varieties of syenites are more or less interrelated to each other in their mineralogy and chemical composition. The syenites of the Sevvattur basin exhibit magmatic continuity with the syenites of the Jogipatti basin. They exhibit a co-magmatic relationship and gradational, zonal, spatial and temporal variations and continuities.

An arc-like vogesite outcrop with a lamprophyric pandiomorphic texture with black needles of katophorite set in a feldspathic matrix of two generations occurs in the Sevvattur basin with close proximity to carbonatite exposures. The vogesite imperceptibly grades to ferro-hastingsite syenite, speckled hornblende syenite and hornblende-biotite oligoclasite. An

acmite-bearing syenite grades with an enrichment of cumulate needles of katophorite into lamprophyric vogesite, displaying a pandiomorphic texture. The shonkinite occurring in Jogipatti basin is a coarse-grained inequigranular rock composed of equal proportions of sanidine / anorthoclase and augite, with accessories of olivine, hastingsite, phlogopite, apatite and magnetite and exhibiting a lamprophyric pandiomorphic texture. In the field, it occurs as xenoliths or nodules in ultramafic rocks. The ultramafic rock which is the host rock of the shonkinite appears to be possessed of kimberlitic affinity (Ramasamy et al., 2010). Mineralogical gradation exists between the shonkinite and garnetiferous syenite. An abrupt mineralogical and compositional gradation exists between the vogesite and shonkinite. Similarly, there exists such gradation between vogesite and hornblende-biotite oligoclasites. Again, the shonkinite exhibits such a type of gradation between the garnetiferous-orthoclase syenite and the mottled augite syenite. On the whole, one syenitic member has genetic relationship with any other member in this zoned complex, either in mineralogical or compositional gradations. In a detailed petrographic and mineralogical study, it is shown that the shonkinite is considered as a parent magma for this carbonatite alkali-syenite complex (Saravanan and Ramasamy, 1995; Ramasamy et al., 2010). Dykes, ring dykes, sills, veins, cavity fillings, cone sheets and plugs of syenites and carbonatites show sharp contacts with chilled margins with their host rocks. Curvilinear tensional cracks are seen around the exposures of the syenites and carbonatites. Late magmatic aplites and pegmatites filled these cracks and show co-magmatic relationships with the adjoining plutons.

All of the carbonatites occurring in the three places in Sevvattur, Jogipatti and Onnakarai grade with zonal variation from ferro-carbonatite, beforsite and sovite. Calcite, dolomite and ankerite constitute the essential minerals in these rocks and biotite, phlogopite, magnetite, riebeckite, aegirine augite, acmite, wollastonite, garnet and the rare-earth minerals of pyrochlore, zircon and niobian rutile constitute the notable accessory minerals in these rocks. Two generations of magnetites, both in the form of opaque dusts and anhedral, euhedral and twinned crystals, are present in some of the carbonatites and in the shonkinite. The Fe- and Mg-rich carbonatites appear to be emplaced from relatively deeper horizons. By their characteristic minerals, the zoned cone-sheets of the carbonatites in Sevvattur exhibit various sheets and layers as hybrid sovite, biotite sovite, phlogopite sovite, aegirine sovite, pyrochlore-bearing para-ankeritic sovite, pyrochlore-rich para-ankeritic beforsite, magnetite beforsite and apatite soviet. The elongated rings and veins of the riebeckite-carbonatites are seen in the riebeckite syenites of the Jogipatti basin. The hybrid carbonatites of the Jogipatti basin are enriched with richterite, magnesio-arfvedsonite, acmite, wollastonite and scapolite. The carbonatites of Onnakarai appear to be younger than the Jogipatti carbonatite, which is intermediate and younger itself than the Sevvattur carbonatite (Ramasamy, 1973). Again, the zoned alkali syenites of Sevvattur are older than those in the Jogipatti basin. A carbonatite body crops out in arcuate cone-sheets with a sharp contact along the meeting between the ultramafic rocks and the syenites in the northern periphery of the Sevvattur body. Mineralogical variations occur as zones which are almost conformable with one another, starting from the convex side of the arc and proceeding to the concave side in the following order: a) micaceous zone, b) ankerite zone, c) beforsite zone and d) sovite zone. About 400 m west of the carbonatite exposure is evidence of the forceful injection of carbonatite, as manifested in a syenitic outcrop which has been thoroughly brecciated with feldspar grains which were twisted and ragged with the emplacement of fine-grained carbonatitic cementing media. Along the contacts of the carbonatite, the host rocks have

been carbonatized by the intrusion of a thin vein in which lots of carbonates and replacements of silicate minerals into calcites are observed. Iron-enriched phlogopite is found at the contact of carbonatite with the ultramafics. Schiller-type inclusions are common and abundant along the cleavages and partings of the augite crystals. Hornblende wraps round the augite and is pleochroic, from green to yellow. Small prisms of biotite are found along the margins of the pyroxene and hornblende. An economical deposit of vermiculite has been formed at the contact between the ultramafics and the carbonatites. The carbonatite exhibits a well-developed concentric flow structure with linear crystals of apatite, alkali-amphibole and magnetite or else a schlieren of hornblende and biotite and streaky patches of ferromagnesian minerals. The carbonatite imperceptibly grades into sovite, beforsite and ankerite, depending upon an increase of dolomite or ferro-carbonates. In the ferro-carbonatites, which are relatively emplaced from deep-seated sources, pyrochlore, ilmenite and ilmenorutile concentrated in the Sevvattur, Jogipatti and Onnakarai villages, respectively. The broad spectrum of the evolution of the carbonatite complex is manifested in: a) introduction of the calcite into the host rocks, b) the formation of calcium-bearing minerals like grossularite-andradite, melanite, wollastonite, richterite paragonite, margarite, sphene and epidote, c) the alkalinization of clinopyroxene and amphiboles, d) phlogopitization and e) feldspathization. The carbonatite exhibits a xenomorphic granular texture by the presence of anhedral calcite or dolomite grains. The oligoclase and potash feldspars in the plates of the calcites of carbonatites are often corroded with an embayed outline. The micro-fractures in the host rocks are filled with calcites and some mafic minerals are transformed into margarite. The potash feldspar is found as inclusion along the contact of carbonatites and syenites and the host rock is enriched with turbid granular potash feldspar. Lumps of granular clinopyroxenes are developed in the host rock of ultramafics along the point of contact with the carbonatites. The grain size of the granular clinopyroxene has been transformed into well-developed clinopyroxene with larger dimensions. Some of them grow to over 10 cm in their dimensions as single crystals. Apatite is the more common accessory mineral in this contact zone. Clinopyroxene and amphiboles are converted into biotite. Wollastonite, garnet (melanite) or scapolite are formed as small prisms interstitial to acmite and appear to be formed by magmatic crystallization (Eckermann, 1966).

Both the basins are surrounded by ultramafic rocks. They include dunite, peridotites, kimberlites, pyroxenite, biotite pyroxenite, massive amphibolites and biotite. It is not possible to classify these rocks in the field owing to their scarce exposure on the surface and so they are together classified as ultramafic rocks. Magnesite and kankar are found on the weathered surfaces of the ultramafics. Dunite and peridotites are altered to talc-steatite and calcite-bearing rocks. Massive dunite exhibits a saccharoidal texture. However, the grain sizes of these rocks vary widely. Porphyritic pyroxenite with kankar veins is also seen in some well sections. Ultramafics rich in biotite and amphibole are very common. Veins and selvages of calcite-bearing riebeckite showing a schistose structure fill the cracks developed within the ultramafics. The ultramafics are essentially comprised of pyroxenites and peridotites. Thin veins of oligoclasites, albitites and carbonatites intrude into the ultramafics, which are transformed into biotite-pyroxenite and hornblende-oligoclase-calcite-bearing pyroxenite. Many varieties of hybrid carbonatites are developed at the point of contact of the ultramafic rocks with the carbonatites. Alkali pyroxenes like aegirine-augite and augite have developed in the ultramafic rocks and in the syenites. Alkali amphiboles like magnesio-riebeckite, magnesio-arfvedsonite and richterite have developed extensively in the aplitic syenites. Grossularite, melanite, scapolite, calcite and wollastonite were

developed at the point of contact with the alkali syenites-carbonatite-ultramafics. Feldspathic selvages in ultramafics often display the development of biotite. At the contact between the garnetiferous syenites and the ultramafics, a skarn rock has been developed at around 2000 m length and with a width ranging from 10 to 200 m. It is comprised of calcite, wollastonite, grossularite and epidote as major minerals. In these rocks, no accessory minerals characteristic of carbonatites, such as apatite, magnetite, zircon, alkali pyroxenes, amphiboles and REE minerals, are seen. The individual minerals in the skarn rock do not have any mineral lineation steeply plunging towards the centre of the basin. However, evidence such as the partial transformation of diopside into calcite, garnet or wollastonite is present for the carbonate metasomatism of one mineral into another. The rock has been extensively folded, sheared and deformed, carrying ultrabasic nodules of varying dimensions from less than 1 cm to over 40 cm. These nodules are partially carbonatized and they exist discontinuously along the folded axial planes. The intricate folding pattern with layers and veins of calcite is even seen in hand specimens. Granulitic and gneissic layers occur within it as contorted and elongated lenses. These knotty inclusions stand out boldly on the weathered surfaces. The skarn rock exhibits a characteristic ribbed structure due to weathering. The ribs are parallel to the foliation direction and are developed along the trend of the elongation of the direction of the relics of mobilized ultramafic nodules towards the N 45° direction. Specks of native copper, bornite, covellite, chalcopyrite, pyrite, galena pyrrhotite are disseminated into the nodules. The modes of the occurrence of these nodules indicate that part of the ultramafic rock occurring along the contact of the garnetiferous syenite has been transformed into a skarn rock during the emplacement of the syenite body along its contacts. Moreover, along these contacts, riebeckite-sovites, acmite and riebeckite-bearing ferro-carbonatites, veins of ferro-carbonatite breccias are seen. The ferro-carbonatite breccia carrying angular fragments of ferro-carbonatite and riebeckite syenite, quartz carrying inclusions of riebeckite needles and euhedral magnetite crystals sets in very fine-grained carbonate matrix. Besides breccias, there are exposures of monazite bearing riebeckite syenite, benstonite carbonatite, barite veins, veins of galena and sulphide hosted aplites and pegmatites are emplaced just inside and on the western outside of the skarn rock exposures. The ultramafic body exposed to the west of the skarn rock is seen with the extensive development of biotite and with specks of sulphide minerals aligned characteristically along the foliation or schistose planes of the rock. It is subjected to vermiculitization with the emplacement of carbonatitic veins. In places, veins of ilmenorutile, barite, apatite-ilmenorutile rock, ankeritic carbonatite and riebeckite are seen in it. The biotite is extensively developed in the ultramafic rock along its contact with garnetiferous syenite. Small pockets of massive biotite-hornblende granites with a sharp point of contact with the country rocks of granite-gneisses occur in the north and south of the carbonatite complex. An arcuate fault-bounded aegirine granite exposure imperceptibly grades towards the east as the hornblende granodiorite in the east is seen in between the two syenite basins. The other granites occurring in this complex also have a gradational variation in their mineralogy and in their chemical compositions, and they also have a genetic relationship with that of the alkali syenites.

8. Zoned carbonatite-alkali complex

The mineral assemblages in the alkaline rocks occurring in the two adjacent basins exhibit continuous chemical variations from one end to the other in various members of co-

magmatic alkaline rocks. Larger syenite bodies show imperceptible gradation to the adjacent syenite bodies. The syenites and carbonatites are composed of both early-formed and late-formed minerals (Saravanan and Ramasamy, 1995). All of these rocks are classified based on their wide variations in their textural features and mineralogical compositions. The mapping was carried out based on these features in the field. The anorthite content in plagioclase feldspars in the syenites varies between An28% and An35%, and often oligoclase is the predominant in the speckled syenite and it decreases to An4% in the places from the mottled porphyritic syenite which imperceptibly grade from that speckled porphyritic syenite with an oligoclase of An18%. Plagioclase growth twins are evident in the syenites. Carlsbad (twin axis {001}, penetration twin), acline(composition plane {001}) Baveno (contact twin, twin plane {021}) and Manebach (contact twin, twin plane {001} twins as well as periclines (twin axis {010}) and albite (twin plane {010}) twins are common in the feldspars of the syenites. Normal zoning (progressively sodic towards the rim) is common and reverse zoning (progressively more calcic towards the rim) is also found, occasionally, in the syenites. In places, the oscillatory normal zonings ranging between An34% and An24% are seen in the speckled syenites. Patchy zonings are found in the biotite syenite porphyries. The anorthite contents of the phenocrysts in the porphyritic syenites, vogesites and the syenite porphyries are slightly higher than those of the plagioclases in the matrix. The potash feldspars have the following mean variations of orthoclase and albite components: speckled hornblende syenite (Or_{77} Ab_{23}), speckled hornblende porphyritic syenite ($Or_{87}Ab_{13}$), mottled augite syenite (Or_{50} Ab_{50}), mottled augite porphyritic syenite (Or_{87} Ab_{13}), shonkinite (Or_{61} Ab_{39}), garnetiferous syenite (Or_{62} Ab_{38}) and riebeckite syenite (Or_{43} Ab_{57}). Microcline cryptoperthite is commonly found in mottled porphyritic syenite and in syenite porphyries. The plot of the percentages of or-ab-an in a trilinear diagram shows that most of alkali feldspars fall within the field of sanidine, anorthoclase, albite and oligoclase. The Al/Si ratios (0.11 in albitite, -0.49microcline-melanite-syenite) in the alkali feldspar appear to be related to the history of the unmixing of the alkali feldspar (Deer et al., 1965). These components are plotted in a diagram constructed for the experimental data under 5000 bars H_2O pressure; they indicate that the individual components fall within the range of 800°C to 950°C (Yoder et al., 1957). Microcline, microperthite, anorthoclase, sanidine and orthoclase are present in various syenite members and show a high degree of triclinicity (ranging between 0.6 and 1.0), indicating its disorder states and their high temperature formations and the emplacements (Ramasamy, 1986) of the syenite bodies. The microcline-microperthite, potassic host ranges from 48% to 67%, while the sodic guest ranges from 33% to 52%, indicating their high disorder relationships and high temperature formations. The feldspars display clouding owing to the presence of very fine dusty inclusions of iron oxides in some varieties of shonkinite and syenites. Such types of clouding are present in calcite, dolomite and in ankerite, with varieties of textural patterns in the carbonatites of Sevvattur. It is interpreted that dissociation of ankerite into calcite and magnetite during the course of the ascension of the magma during successive emplacements of cone sheets of carbonatites from deep-seated sources through the centre of the magmatic body at the late magmatic stages would have produced such textural variations (Ramasamy et al., 2001).

The diopside in pyroxenite and feldspar syenites adjacent to the carbonatite exposures are transformed into calcite. The ultramafic body in the Jogipatti basin is extensively deformed and carbonatized. the proportions of plagioclase content decrease towards the centre of the mottled porphyritic syenite. The colour index (Rittmann, 1973) for the syenites varies widely in the alkaline rocks, depending upon the degree of fractionation and the separation of the

clinopyroxenes or mafic minerals during the course of magmatic differentiation. According to the volume proportion and mineral structure of the mafic minerals present in the various alkaline members, they are subjected to transformations of clinopyroxenes into amphibole, biotite or magnetite. There exists continuity in the compositional variations of the mafic minerals from one syenite member to another (Ramasamy, 1986a). The clinopyroxenes from the youngest alkali syenites fall into the fields of ferrosilite and the calcium-rich hedenbergite end. The clinopyroxene from the melanite-orthoclase syenite contains a high content of CaO owing to the partial transformation of the clinopyroxene into grossularite-andradite garnet (Saravanan and Ramasamy, 1995). During late magmatic stages, due to increase of agpaitic coefficient {(Na+K)/Al} with progressive depletion of Al, orthoclase transforms into highly disordered microcline incorporating ferric iron in its lattice. Release of Ti^{iv} and Fe^{iii} in the appropriate sites of orthoclase and grossularite-andradite garnet as per the exchange of $Ti^{iv}Fe^{iii} \leftrightarrow Ti^{lv}Al^{iii}$ from subsolidus garnetiferous orthoclasite transforms to melanite-microcline syentite (Ramasamy, 1986). Owing to increasing crystallization and the transformation of mafic minerals into alkaline mafic minerals, it is also dependent on the mineral proportion of mafic minerals present in the individual alkaline rocks. Replacing Ca ions from the amphiboles of $Ca_{76}Na_{15}K_9$ by the substitution of (Na+K) in the M4 sites of the amphiboles to $Ca_{27}Na_{65}K_8$ in the younger generation of syenites caused the crystallization of the riebeckite. Furthermore, the ratio of 100 Mg/(Mg+Fe+Mn) of the calciferous amphiboles decreases from 85 to 30% because of the changing composition from pargasite to ferrohastingsite in the younger syenites. The katophorite and richterite are restricted to vogesite and hybrid carbonatites respectively. The eckermannite, magnesio-arfvedsonite, arfvedsonite, magnesioriebeckite and riebeckite are widely distributed in potash rich syenites and carbonatites. Both the clinopyroxenes and amphiboles are deficient in Si in their tetrahedral sites and are compensated by Al and Ti ions. However, under increasing P_{H2O} in the late magmatic syenites, Si is saturated and Na replaces Ca with increasing silica activity. The "m" value of biotite Mg/(Mg+Fe) decreases from 0.91 to 0.29 in the late magmatic syenites. The Cs (4-10 ppm), Rb (30-345 ppm) and Li (1.5-7.5 ppm) contents increase as K increases in this complex.

The emplacement of younger alkali syenite bodies at the contacts of older syenite units plays a critical role in the transformation and metasomatism of mafic minerals into alkali-rich minerals. Again, feldsic minerals are also subjected to metasomatism, such as the transformation of oligoclase into potash feldspars. The oligoclase surrounded by the rims of reverse zoning in the mottled porphyritic syenite indicates that it is ascending to higher levels. The presence of peristerites formed by the sub-microscopic intergrowth of sodium-rich and calcium-rich phases is observed in the mica syenite porphyries. The compositional zoning indicates that with a decrease of the temperature, the sequence solidified from the margin inwards. However, such metasomatism appears to take place at sub-solidus phases of the phenocrysts through the escape of volatile constituents carrying the required ions in the vapour or liquid phases. Sheets and plugs emplaced at the inner portions appear to be derived from a deep-seated magmatic column. The solidification was interrupted repeatedly by surges of fluid core magma. The emplacements of the various plutons are structurally controlled. The isoclinal folding of the flow bands of the carbonatitic or syenitic layers were developed, indicating the stretching and spreading of the carbonatitic or syenitic magma along the narrow zones of the emplacements. The residual magmas formed through the differentiation and fractionation of a shonkinitic parent magma resulted in decreasing silica

activity and steadily increasing oxygen fugacity and agpaicity due to the progressive enrichment of alkalis, ferric iron and volatile constituents in a closed magmatic chamber (Saravanan and Ramasamy, 1995). The relative rate of the development of agpaicity in the residual liquid and the crystallization of femic and felsic minerals also played a critical role in the alkaline magma's evolution. The silica deficiency developed in the residual magma due to the early crystallization and fractionation of the clinopyroxene and alkali feldspar, which may have been compensated for through the formation of amphibole, biotite, carbonates, phosphates and magnetites (Yagi, 1953). Therefore, all of these magmatic bodies exhibit compositional zonings. The compositional zoning indicates that, with a limited decrease in the temperature, the sequence solidified from the margin inwards. Sheets and plugs emplaced at the inner portions appear to be derived from a deep-seated magmatic column. The emplacements of the various plutons are structurally controlled.

The early-formed clinopyroxene in some of the syenites reacted with the residual magma and transformed into calcic-rich diopside and then into augite and aegirine-augite to acmite. Similarly, the acmite transformed into garnet which, again, transformed into melanite with an enrichment of titanium. the calcite reacted with silica-forming wollastonite in the garnetiferous syenite and it reacted with plagioclase forming scapolite, taking the required amount of SO_3 from the volatile phase enriched with this constituent (Tables 2 and 3), as revealed from the chemical analyses by the enrichment of SO_3 in bulk rock compositions. The quartz content decreases from the rocks outcropping at the outer shell to those rocks occurring towards the centre of the Sevvattur basin. On the other hand, such variation is remarkable given the formation of riebeckite, biotite, magnetite, wollastonite, garnet, melanite, scapolite and calcite by the heteromorphic transformation of mineral assemblages to compensate for the silica deficiency of the residual magma impoverished in the silica owing to the crystallization of sodaclase anorthoclase, sanidine and high temperature microclines in the syenites of the Jogipatti basin. The enrichment of volatile constituents like H_2O, CO_2, SO_3, P_2O_5 and F in the late magmatic residual magmas developed different varieties of oxide minerals, like magnetite, rutile, ilmenorutile, perovskite and zircon, carbonate minerals like calcite, dolomite, para-ankerite, benstonite, sulphate minerals like barite, gypsum and scapolite, phosphate minerals like apatite and monazite, and sulphide minerals like galena, chalcopyrite, pyrite and pyrrhotite. The very presence of these minerals indicates that the residual magma was enriched in these volatile constituents, which compensates for any silica under-saturation owing to the extensive development of feldspathic constituents. Most of the rocks in this complex have insufficient alumina to form adequate alkali feldspars. The emplacements of carbonatites and its co-magmatic alkali syenites are in a sequential order due to a series of pulses occurring during intermittent tectonic disturbances.

Olivine is present in significant proportions in ultramafic rocks, shonkinite and carbonatites. The compositions of olivine in the ultrabasic rock represent an intermediate position in the course of the magmatic evolution of the olivine occurring in the shonkinite. The olivine in the shonkinite exhibits peripheral zonal variation augite, aegirine-augite and jadeite, indicating a prolonged period of crystallization under the liquid stage. The high concentration of Ca-Na-K-Al in the olivine from the ultramafics indicates its kimberlitic affinity. These features indicate that shonkinite magma is the parent magma for the ultramafics. The early fractionated olivine from the parental shonkinite magma reacts with the residual magma and the peripheral portion of the olivine is transformed into diopside

on slow cooling with release of volatile constituents into the residual magma, inducing magmatic pressure by incorporating CaO. The crystallization of the clinopyroxene in the place of the olivine, the residual magma, is depleted in the silica. Under increasing magmatic pressure and in order to meet the silica deficiency, more Na_2O and Al_2O_3 are incorporated with the development of aegirine augite. With the impoverishment of SiO_2 and Fe_2O_3, jadeite crystallizes from the residual magma along the peripheral portion of the olivine or the clinopyroxene. The jadeite develops along the peripheral portions of the olivine within the temperature range of 600 to 800°C with a pressure ranging from 10 to 20 kbar under progressive enrichments of Al_2O_3 and Na_2O and with decreasing silica activity in the residual magma (Ramasamy et al., 2010). The crystallization of jadeite (jd) in the place of albite (Ab) or nepheline (Ne) compensates the silica deficiency in the residual magma.

$$2jd \leftrightarrow Ne + Ab$$

The further crystallization of jadeite - the residual magma - is enriched with K_2O, Al_2O_3 and SiO_2 (Yagi, 1953).

Thus, the development of jadeite produces as end products silica under-saturated nepheline-free shonkinite with the crystallization of potassium feldspars from the residual magma. With an increase of the vapour pressure during the late magmatic processes, particularly under high P_{CO2}, the mafic cumulates become unstable and release more CaO into the melt. The Ca-enriched residual magma immiscibly separates into silicate and carbonate magmas under high P_{CO2}. The further differentiation of these magmas produces a series of alkali syenites and carbonatites, successively emplaced in a sequential order, first in the Sevvattur basin and then in the Jogipatti basin, and resulting in the formation of the zoned alkali carbonatite complex of Tiruppattur, Tamil Nadu.

Normally, a carbonatite complex is associated with alkaline rocks accompanied with significant amounts of alkali-rich ferro-magnesium minerals. Often, a fenitized aureole is present around the carbonatite complex owing to the alteration of country rocks by its reaction with alkali fluids escaping from the carbonatite body. The country rock may be changed into silica-impoverished nepheline-bearing fenites. In this complex, such a development of fenites is absent. As magmatic differentiation takes place within a closed magmatic chamber for a prolonged period of crystallization and differentiation, the alkaline fluid evolves during the course of magmatic evolution, reacting with the minerals and crystallizing from the magma and increasing the alkali constituents up to the development of ultrapotassic syenites. The transformation of diopside into acmite and jadeite during the course of magmatic evolution is adjusted with the development of acmite (Fig. 2) and the ensuing silica deficiency is compensated for by the reaction of albite with silica under-saturated residual magma forming a jadeite component. Under high oxygen fugacity and a volatile concentration, biotite and magnetite form in the place of jadeite. The distribution of volume proportions of alkali feldspar against quartz (Fig. 3a) and alkali feldspar against plagioclase is calculated on the basis of the Rittmann norm using the chemical analyses listed in Tables 1 and 2 for the plot in the Q-A-P-F (Rittmann, 1973) diagram, indicating a linear differentiation trend for co-magmatic alkali series of rocks (Fig. 4 a & b). In Fig. 5a-j, it is indicated that the distribution of major elements in binary variations indicate overlapping smooth linear trends for syenites, ultramafics, carbonatites and dolerites. The dolerites in this area also show a trend of alkali-enrichment during its magmatic evolution.

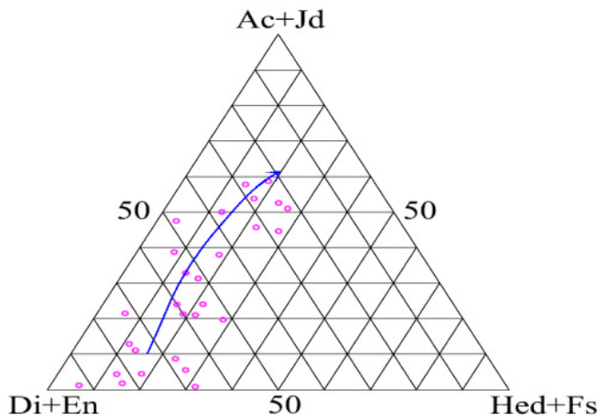

Fig. 2. The chemical compositions of alkaline rocks calculated on the basis of Acmite+Jadeite, Diopside+Enstatite and Hedenbergite+Ferrosalitse compositions, indicating a magmatic differentiation trend moving towards the Ac+Jd end members. The diagram indicates the enrichment of alkalis and iron during the course of differentiation

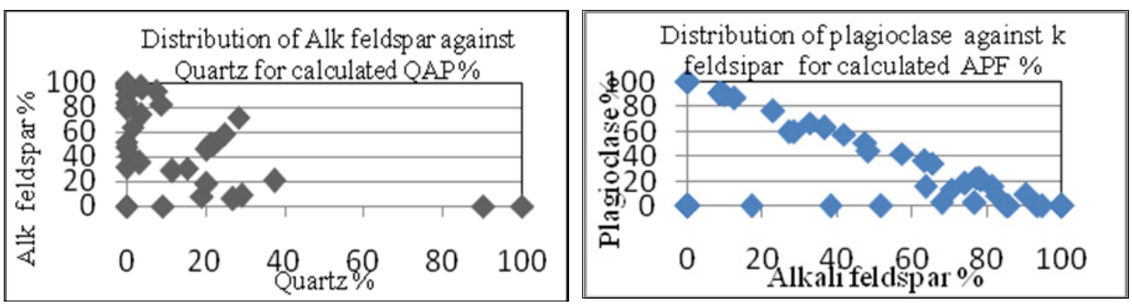

a) b)

Fig. 3. a. & b. Streckeisen (1967) QAPF double triangle plots are presented in Qz-alk-felds and Alk-felds – Pl variation diagrams showing linear variations in co-magmatic series (The C.I. for syenites varies from 5-30; for hybrid rocks 30-70; for ultramafics 70-100).

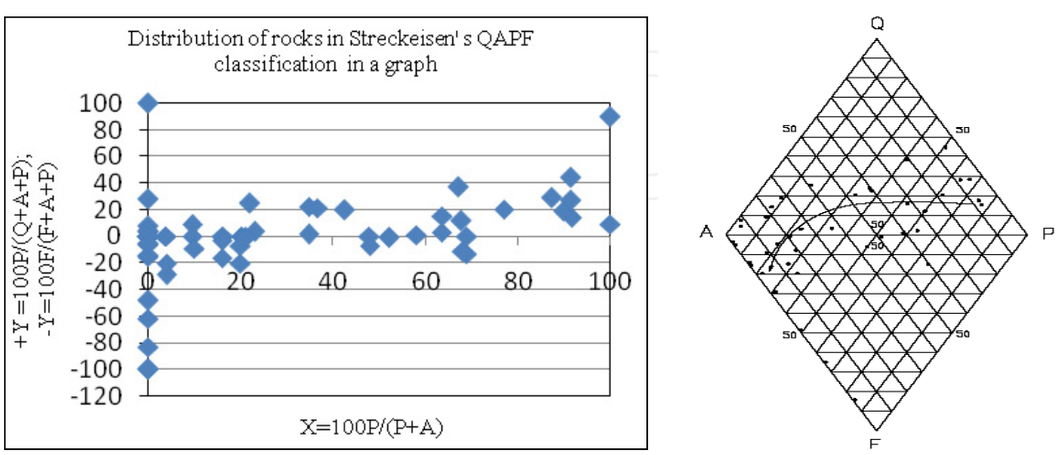

a) b)

Fig. 4. a., b. Streckeisen graph and double triangle showing the linear trends of the magmatic evolution of alkaline rocks in the Tiruppattur carbonatite complex

Rock	No	SiO2	Al2O3	Fe2O3	FeO	MnO	MgO	CaO	Na2O	K2O	TiO2	P2O5	CO2	SO3	H2O
Bio oligoclasite	723	48.35	12.97	3.78	3.26		2.68	12.91	3.54	5.00	0.75	1.06	2.76		3.15
Bio fol aplite	1122	50.28	23.25	5.54	2.98	0.36	3.82	5.60	2.08	1.80	0.90	0.60	0.60		
Bihbpor syenite	428	51.53	18.22	7.53	2.79		4.00	7.50	3.85	2.70	0.65	0.22	0.39		0.44
Vogesite	733	53.07	13.03	4.28	5.09		3.75	11.75	4.00	3.93	0.69	0.48			0.36
Aughb syemite	464	53.17	14.06	5.32	5.42	0.35	3.62	9.06	3.80	2.25	1.30	1.50			0.68
Ac albitite	468	54.37	5.30	19.84	1.95	0.52	0.98	2.50	11.75	0.80	1.50	0.36			0.46
Bihbpor syenite	370	54.44	17.80	4.63	3.82	0.34	2.71	5.90	3.80	3.60	0.65	0.85			0.95
Augpor syenite	459	57.72	18.18	1.75	2.24		2.38	7.90	4.15	4.10	0.28	0.46			0.34
Augpor syenite	476	58.16	17.98	2.88	2.70		1.87	5.98	3.69	4.70	0.65	0.82			0.39
kato syenite	18	58.18	17.19	2.64	3.19	0.17	1.36	6.36	5.40	4.08	0.69	0.29			0.20
Augpor syenite	485	58.58	11.14	3.47	3.01	0.30	2.97	8.37	4.84	3.50	0.70	1.48	0.21		1.20
S.concave syenite	34	59.59	20.67	0.74	0.28		0.01	0.01	4.86	8.66	0.01	0.01	0.29		0.07
Albitite	461	60.87	14.09	0.32	2.62	0.40	2.51	4.14	8.00	2.57	0.20	1.81	0.51		1.58
Sev gar peg syenite	43	61.25	20.76	1.78	0.28		0.01	1.98	10.62	0.65	0.01	0.01	1.08		0.07
Kakangarai syenite	7	61.26	20.91	0.89	0.53		0.01	1.10	4.67	8.84	0.01	0.01	0.25		0.10
Sevvattur syenite	10	62.22	20.98	1.14	0.28		0.01	1.44	4.54	9.07	0.01	0.01	0.48		0.08
SevNE syeite	36	62.68	19.41	1.17	0.13		0.01	0.93	9.07	3.15	0.01	0.01	0.62		0.03
Kunnattur syenite	3	63.05	22.39	0.43	0.28		0.01	0.67	8.55	4.00	0.01	0.01	0.44		0.05
Koratti syenite	44	63.53	20.60	0.59	0.27		0.01	0.40	7.77	6.96	0.01	0.01	0.40		0.02
Karapattu syenite	6	63.54	22.27	0.74	0.27		0.01	0.75	8.55	2.86	0.01	0.01	0.30		0.09
PinkBihbporsy	463	64.24	14.74	2.84	2.02	0.83	1.13	2.42	4.93	3.34	0.62	0.52	0.44		1.43
Bi-ab-peg syenite	635	67.01	14.06	3.99	1.98		0.52	2.38	6.77	1.40	0.15	0.81	0.34		0.20
Bi hb syenite	369	70.30	13.35	1.94	2.63	0.20	1.17	4.05	3.36	1.58	0.45	0.62			
Richteite ultramafic	321	21.02	1.64	5.48	2.87	0.63	6.39	31.68	1.96	1.44	0.45		23.65	0.69	0.65
pl px ultramafic	319	41.26	3.65	10.18	8.26	0.29	9.67	20.18	0.41	1.20	1.48	0.73	0.41	0.34	1.15
bi-fels px ultramafic	320	44.12	9.10	3.64	1.26	0.06	14.20	21.78	1.15	1.24	0.88	0.10	1.12		0.60
gar pegmatite	572	44.84	11.35	12.14	0.50	0.40	0.70	19.01	3.95	4.98	0.40	1.20			0.40
px hb bi ultramafic	203	45.82	15.53	1.50	5.59	0.19	3.95	9.62	5.27	5.16	0.66		4.66	0.14	1.80
hb oligo ultramafic	204	49.16	21.03	2.57	5.16	0.08	5.43	12.37	2.43		0.83		0.14	0.16	0.30
Shonkinite	561	49.20	7.61	6.40	5.58	0.36	10.43	10.03	3.44	4.29	0.76	0.82			0.80
Olaipatti syenite	78	51.94	22.27	3.53	0.41	0.14	0.01	4.50	0.92	13.54	0.01	0.01	0.93		
gar aplite	39	52.28	19.59	2.82	1.73	0.13	0.25	5.15	0.14	17.16	0.56	0.13			0.44
bi px ultramafic	318	52.92	12.98	5.31	1.80	0.11	3.21	6.18	2.03	11.76	1.09	0.46	2.24	0.16	0.44
Olaipatti syenite	75	53.43	19.31	6.94	0.28		0.01	7.58	2.35	7.72	0.01	0.01	0.93		
Olaipatti syenite	77	54.25	22.99	2.83	0.56		0.01	2.12	2.44	12.05	0.01	0.01	1.04		
Olaipatti syenite	79	54.60	23.21	4.05	0.55	0.16	0.01	5.70	1.93	8.84	0.01	0.01	1.04		
Bi-mus oligoglacite	219	55.02	18.75	2.17	0.36	0.03	1.24	4.47	3.31	10.32	0.28		2.54	1.30	1.30
hb syeite	361	56.84	15.69	2.37	3.02	0.17	1.73	7.73	3.24	6.96	0.50	0.47	0.44	0.76	0.82
aplite	201	58.50	18.65	3.11	0.85	0.07	0.49	2.75	6.48	6.24	0.44		0.30	0.13	1.00
Jogipatti syenite	51	58.92	19.14	1.89	0.56		0.01	1.20	1.09	14.68	0.01	0.01	1.00		
anorthoclasite	349	58.98	16.20	2.51	2.72	0.12	2.22	5.15	6.75	3.48	0.56	0.17	0.22	0.74	0.50
Rieb gar pegmatite	360a	59.78	18.27	1.32	1.14	0.07	1.21	5.61	5.40	6.78	0.20	0.17			0.10
Bi pegmatite	340	61.82	16.90	0.61	0.34	0.02	0.49	2.06	0.27	16.80	0.09		0.42	0.25	0.32
Garigaipalli syenite	85	62.69	20.15	0.21	0.14		0.01	0.01	1.43	15.06	0.01	0.01	0.19		
bihb oligoclasite	206	63.18	15.02	2.73	4.39	0.14	2.72	5.50	3.98	1.32	0.66		0.30		0.38
rieb pegmatite	301	63.24	17.74	0.88	0.72	0.03	0.49	2.41	4.73	10.12	0.28			0.15	
rieb pegmatite	85	63.75	13.01	1.98	0.65		2.59	0.89	5.21	9.98	0.10	0.40			1.10
rieb aplite	541	64.01	15.44	2.44	0.25	0.40	1.62	0.21	4.04	9.15	0.14	0.22			1.58
Rieb diorite	80	64.97	16.75	2.61	1.31	0.40	0.53	3.75	5.04	2.70	0.30	0.48			0.82
Rieb sy pegmatite	36a	65.01	17.66	1.25	0.57	0.03	0.49	2.41	7.02	4.92			0.16	0.05	0.20
Pink granite	12	69.72	14.92	1.40	0.71	0.07	0.71	3.15	4.79	4.32	0.31				0.48
Pink granite	1	70.20	14.42	1.94	0.57	0.04	0.47	3.09	4.19	4.74	0.40	0.16			0.62
Rieb granite	78	71.40	13.60	2.53	0.63	0.50	0.72	2.67	3.80	2.93	0.15	0.32			0.52
ap-mt rock	498	0.48	0.73	54.17	18.07	0.49	0.73	6.66	0.14	0.42	13.20			0.77	
barite rock	452	0.50		0.10			0.05	0.50	0.05				0.53	33.40	0.80
apatite rock	450	2.06	6.91	2.89	2.06	0.07	1.46	41.36	0.47	0.10	10.01	31.77			0.26
Crocidolite rock	60	6.50	1.09	0.49	0.26	0.09	0.85	50.84	0.01	0.01	1.68	0.02	37.86		0.00
Ultramafic	460	18.84	0.91	28.94	17.60	0.19	5.42	15.42	0.06	0.14	3.15	3.00	4.50	0.30	1.30
Feore rock	13	20.36	0.07	27.60	37.85	0.46	0.01	11.16	0.71	0.34	1.57	0.04			
Ultramafic	492	27.72	0.80	16.25	7.15	0.78	6.37	19.09	4.04	0.28	0.60	0.21	15.26	0.23	0.36

Sevvattur syenites No723-369; Jogipatti syenites No 321-36a; Granites No12-78; Ultramafics No 498-47; Carbonatites No 310-495; Dolerites No 1176-1224

Table 1. Chemical composition of the alkaline rocks in the carbonatite complex of Tiruppattur

Rock	No	SiO2	Al2O3	Fe2O3	FeO	MnO	MgO	CaO	Na2O	K2O	TiO2	P2O5	CO2	SO3	H2O
Peridotite	31	30.09	2.00	19.09	6.95	0.79	9.91	15.68	3.67	0.01	0.63	1.29	8.93		
Biofels pyroxinite	9	36.88	1.47	15.49	10.72	0.10	8.00	17.76	1.53	1.88	1.74	1.97	1.10		
Kimberlite	29	37.71	0.12	8.46	3.29	0.15	8.71	21.10	0.32	2.93	0.75	0.09	16.60		
Samalpatti ultramafics	S3	38.09	5.17	1.05	14.10	0.18	14.18	15.52	0.23	3.44	1.66	3.69			1.90
Feore rock	21	39.30	0.07	49.84	10.36	0.02	0.01	0.01	0.16	0.17	0.33	0.14			
Kimberlite	7a	40.85	0.74	10.33	0.57	0.13	19.08	7.00	0.40	0.01	0.01	0.01	20.65		
Riebcc ultramafic	491	42.36	1.27	7.54	1.98	0.19	12.97	15.65	4.59	0.90	0.44	0.10	9.75		2.15
Olaugoligo ultramafic	40	42.58	4.62	6.32	5.25	0.15	10.62	25.08	0.34	0.06	0.93	3.10	0.60	0.33	0.60
apatite rock	451	42.82	1.27	21.86	2.51	0.04		14.76	1.95	0.06	1.56	7.90	2.46	1.65	0.24
Samalpatti ultramafic	S4	45.21	1.28	0.90	4.32	0.09	14.82	20.00	2.34	0.28	0.23	0.05	9.68		1.10
Ultramafic nodule	497	45.92	6.12	5.52	5.33	0.18	9.60	22.46	1.08	0.18	1.26	0.19	1.02		0.50
Rieb ultramafic	402	46.40	10.41	9.31	2.87	0.22	8.32	12.42	3.04	4.38	0.84	0.44	0.17	0.55	
Sam ultramafics	S5	46.41	2.09	1.64	2.90	0.10	14.46	18.90	2.55	0.74	0.17	0.74	8.73		1.08
Sev Ultramafics	S1	46.77	2.17	3.43	12.58	0.13	14.02	19.76	0.19	0.35	0.66	0.33			
wollastonite rock	491	49.66	1.22	2.01	0.63	0.67	1.52	41.86	0.34	0.30	0.07	1.15	0.30	0.30	0.20
Biopx ultramafic	736	52.40	12.26	2.99	6.75	0.02	6.01	8.48	3.11	4.26	0.99	1.53	0.49		0.00
Sam ultramafics	S2	54.65	1.01	0.85	4.12	0.15	17.17	21.37	0.44	0.12	0.22		0.02		
Fe ore ultramafics	47	62.14	0.17	33.58	1.22	0.01	0.01	1.07	0.01	0.34	1.30	0.01	0.39		
Sev carbonatite	310	0.20	0.18	3.60	2.97	0.55	17.40	29.54	0.10	0.60	0.10	0.05	43.56		0.50
Icelandspar	499	0.28	0.08		0.14		0.25	55.03	0.21	0.12	0.14		43.04		0.50
Sev.carbonatite	11	0.30		0.12		0.06	3.84	52.12	0.10	0.05			43.10		0.20
Sev. Carbonatite	59	0.50	0.29	1.25	1.38	0.48	5.00	45.59	0.46	0.07	0.40	1.30	41.45		1.10
Sev carbonatite	389	0.60	0.79	1.23	3.29		15.28	32.28	0.50	0.10	0.10	2.33	42.35		0.40
Sev carbonatite	250	1.00	0.70	4.08	0.60	0.06	0.45	50.46	0.34	0.22	0.20	0.82	39.28		0.50
Sev.carbonatite	410	1.26	0.42	5.00	1.33		4.52	45.46	0.68	0.43	0.15	1.80	39.10		0.28
Jogi. carbonatite	313	1.88	0.65	3.55	2.36	0.62	11.25	36.04	0.20	0.09	0.15	0.02	40.02	1.66	0.40
Jogi.carboatite	315	2.06	0.60	3.90	2.93	0.60	13.23	32.51	0.37	0.33	0.10	0.04	40.24	1.35	0.45
Jogi.carbonatiate	311	2.64	0.50	1.10	0.42	0.50	2.45	48.28	0.20	0.13	0.20	0.04	40.46	0.57	0.32
Jogi. carbonatite	990	3.24	0.94	2.30	0.41		1.06	48.43	2.30	0.50	0.20	1.48	38.52		0.52
Sev.carbonatite	369	4.90	2.95	4.62	0.95		12.29	32.24	0.73	0.08	0.20	1.66	38.14		0.44
Sev. carbonatite	20	9.97	5.06	0.88	2.35		3.12	46.90	1.10	0.57	0.30	2.01	26.32		1.00
Onna Bens carbonatite	500	12.51	5.73	2.05	0.13	0.16		24.39	1.05	0.98			27.17		0.59
Jogi carbonatite	321	21.02	1.64	5.48	2.87	0.63	6.39	31.68	1.96	1.44	0.45		23.65	0.69	0.65
Jogi. carbonatite	1010	24.70	2.01	2.54	2.00	0.30	7.06	33.51	2.92	0.90	0.20	3.68	19.45		1.20
Onna carbonatite	496	27.26	1.92	16.11	7.09	2.46	4.91	17.16	3.58	0.24	1.23	1.26	16.34		0.95
Onna.carbonatite	492	27.72	0.80	16.25	7.15	0.78	6.37	19.09	4.04	0.28	0.60	0.21	15.56	0.23	0.36
Onna.carbonatitae	495	41.36	1.45	11.16	5.30	0.32	8.32	13.61	5.20	0.24	0.98	0.52	10.95		0.20
dolorite	1176	47.22	18.44	1.30	9.76	0.38	7.19	11.09	1.68	0.68	0.75	0.40			0.80
dolorite	1155	48.08	19.06	2.30	9.41	0.15	5.42	10.01	2.52	0.90	1.25	0.50			0.38
dolorite	1159	48.58	15.49	1.60	12.80	0.40	4.68	7.80	2.92	0.90	2.60	0.93			0.84
dolorite	33	49.50	15.25	1.67	9.01		7.23	11.85	2.60	0.20	0.53	0.68	0.33		0.62
dolorite	1186	54.18	12.76	1.80	8.80	0.15	8.96	8.20	2.08	0.90	0.85	0.23			0.63
dolorite	1187	55.13	8.46	3.32	9.98	0.30	7.21	9.04	3.36	1.33	1.65	0.12			0.20
dolorite	1224	56.04	8.26	3.21	9.62	0.20	4.61	8.41	6.02	1.58	1.10	0.31			0.55

Table 1. Chemical composition of the alkaline rocks in the carbonatite complex of Tiruppattur (continued)

9. Geological setting and tectonomagmatic evolution

The location of the Precambrian carbonatite complex of Tiruppattur in the Indian peninsula along the Eastern Ghats Paleo-rift System (Ramasamy, 1982, 1987), extending over a stretch of 3000 km x 200 km from Cape Comorin / Palghat Gap to the Brahmaputra valley (Eastern Syntaxes of the Himalayas), is favourable site for a low degree of the partial melting of alkali-enriched upper mantle rocks from a low velocity zone (Schleicher et al., 1998). The rift

system is a superimposed structure over which a series of older block-faulted horsts and graben structures are comprised of a number of magmatic emplacements of charnockites, anorthosites, alkaline rocks, carbonatites and volcanic effusives. It is also favourable for the genesis of under-saturated alkaline magma charged with relatively more anhydrous volatiles (such as CO_2, SO_3, P_2O_5, F, Cl and CH_4 etc.) with respect to H_2O vapour, which is the main constituent in the volatile phase derived from a deep-seated source. The $Mg/(Mg+Fe^t)$ ratios of the magmatic melts are frequently used as an indicator of whether a melt could be a partial melting product of a mantle material. The high mg values between 0.76 and 0.86 in this area depend on the TPX and the volatile constituents by which they were formed; moreover, these ratios of the starting material of the partial melts from the mantle may fall between the ratios of 0.9-0.3 (Mysen, 1975). Accordingly, all of the rocks in this complex can be derived from the partial melts from the mantle horizons. The propagation and penetration of the Eastern Ghats Paleo-rift system by reactivations during the subsequent tectonic episodes from the Early Proterozoic Period may extend to different depth levels, causing certain low degrees of partial melting which have been attained only after some prolonged period of tectonic deformation. According to Ramasamy (1982), a span of charnockitic activities extends from 3100 Ma to 2600 Ma, with anorthositic events extending from 2000 Ma to 1100 Ma and alkali syenitic- carbonatitic activities commencing from 1200 Ma onwards (Ramasamy, 1981). It seems that successively younger magmatic episodes were formed under more anhydrous- and alkali-rich environments and at deeper levels than the older ones, owing to the deeper penetration of the rifted continental plates into the mantle. The emplacement of most of the carbonatites from the Proterozoic to recent periods occurring in various parts of the world is restricted along deep crustal fractures that were controlled by regional structures and tectonics. According to Macintyre (1975), the ages of carbonatite complexes younger than 200 Ma indicate that many of them are intimately related with major changes in plate motion which were globally synchronous. The continental plate formed by the propagation and penetration of the Eastern Ghats Paleo-rift system led to the later separation of Gondwana Land from Peninsular India. The wide-spread Deccan Trap volcanic activity covered more than 500000 km^2 and the thickness of the lava flows exceeds 2000 m in some places (Krishnan, 1962), with younger eruptions of olivine-tephrite, soda-trachyte and carbonatite eruptions at Kudangulam near Cape Comorin indicating that Peninsular India is prone to repeated volcanic and magmatic activities (Ramasamy, 1987) and are also bearing evidence of Indian plate movement towards the north after the break of Antarctica from Peninsular India. The ascension of magma and its rate of cooling, pressure and the volume of volatile constituents played a critical role in the magmatic evolution of the residual magma under a specific geological setting and tectonic movement. The influence of local variations in the TPX conditions during the course of the crystallization of minerals creates complexities in tracing the trends of magmatic evolution in a spatial order. There exists a compositional relationship between these new discrete minerals in younger plutons with the minerals in older plutons in this area. The distribution of incompatible HFSE of K, Ti, P, Zr, Nb, Ba, Sr (Table 4) in these rocks and high ratios of HFSE such as Ti/P, K/(K+Na), Nb/Ta, Zr/Hf, Sr/Ba, LREE/HREE and the presence of minerals like allanite, zircon, apatite, monazite, pyrochlore, niobian rutile, magnetite, galena and feldspars, indicate that the low degree of partial melts from the mantle horizon and the parent magma

separated from the melt were derived from HFSE-enriched portions of the mantle during the folding and up-arching of the mantle rock at a depth there by enriching the above characteristic elements just prior to the initial stage of the rifting of the diverging continental plates of the Eastern Ghats Mobile Belt.

Mineral	SiO2	Al2O3	Fe2O3	FeO	MnO	MgO	CaO	Na2O	K2O	TiO2	BaO	SrO	P2O5	CO2	SO3	F	H2O	H20	Total
Wollastonite	49.66	1.22	2.01	0.63	0.67	1.52	41.86	0.34	0.30	0.07	0.00	0.00	1.15	0.20	0.00	0.00	0.00	0.00	99.63
Epidote	37.72	17.61	4.67	0.18	0.06	2.29	34.34	0.41	0.84	0.96	0.00	0.00	0.07	0.58	0.00	0.00	0.00	0.00	99.73
Apatite1	0.05	0.18	0.00	0.00	0.00	0.52	54.25	0.30	0.00	0.00	0.00	0.80	39.80	0.00	0.00	0.00	0.00	0.00	95.90
Apatite 2	0.22	0.06	0.00	0.00	0.00	0.17	54.15	0.29	0.00	0.00	0.00	1.51	40.03	0.00	0.00	0.00	0.00	0.00	96.43
apatite 1a	0.00	0.00	0.00	0.00	0.00	1.51	55.73	0.00	0.00	0.00	0.00	0.00	40.95	0.00	0.00	1.56	0.00	0.00	99.75
apatite2a	0.00	0.00	0.00	0.00	0.00	1.51	53.28	0.00	0.00	0.00	0.00	0.00	37.96	0.00	0.00	0.80	0.00	0.00	93.55
apatite 450	2.06	6.91	2.89	2.06	0.07	1.46	41.36	0.47	0.00	0.00	0.00	0.00	41.50	0.00	0.00	1.70	0.26	0.00	100.74
Magnetite 498I	0.10	0.18	67.64	22.57	0.39	0.25	1.05	0.00	0.00	8.10	0.00	0.00	0.00	0.00	0.00	0.00	0.00	0.00	100.28
magnetite 498ii	0.72	0.73	54.17	18.07	0.49	0.73	6.66	0.14	0.42	0.00	0.00	0.00	0.00	0.44	0.77	0.00	0.22	0.00	83.56
Iceladspar	0.36	0.00	0.14	0.00	0.00	0.25	55.03	0.21	0.12	0.14	0.00	0.00	0.00	43.04	0.34	0.00	0.00	0.00	99.63
calcite cc250	2.00	0.00	5.40	0.50	0.06	0.25	51.36	0.24	0.12	0.00	0.00	0.00	0.00	40.28	0.00	0.00	0.00	0.00	100.21
dolomite cc310	0.38	0.00	3.80	2.87	0.55	18.40	30.54	0.10	0.60	0.00	0.00	0.00	0.00	46.06	0.00	0.00	0.00	0.00	103.30
calcite cc311	3.74	0.00	1.40	0.32	0.50	2.25	48.52	0.10	0.03	0.00	0.00	0.00	0.00	40.46	0.57	0.00	0.00	0.00	97.89
Carbonatite cc3	36.40	0.00	2.00	0.25	0.37	1.50	31.93	0.17	0.18	0.00	0.00	0.00	0.00	26.62	0.41	0.00	0.00	0.00	99.83
Mg calcite 313	2.78	0.00	4.05	2.16	0.62	11.65	36.44	0.10	0.09	0.00	0.00	0.00	0.00	41.02	1.66	0.00	0.00	0.00	100.57
carbonatite 314	35.30	0.00	1.70	0.36	0.49	1.12	32.72	0.07	0.11	0.00	0.00	0.00	0.00	26.34	0.67	0.00	0.00	0.00	98.88
ferrocarbonate c	3.26	0.00	4.30	2.73	0.60	13.63	33.31	0.27	0.23	0.00	0.00	0.00	0.00	41.84	1.35	0.00	0.00	0.00	101.52
ferrocarbonate 4	53.02	0.00	6.25	1.15	0.20	3.37	19.09	0.04	0.08	0.00	0.00	0.00	0.00	15.56	0.29	0.00	0.00	0.00	99.05
ferrocarbonatec	49.74	0.00	2.25	0.00	0.42	1.00	23.25	0.04	0.11	0.00	0.00	0.00	0.00	19.92	0.60	0.00	0.00	0.00	97.33
ferrocarboate49	49.82	0.00	2.50	0.00	0.23	1.25	23.95	0.04	0.11	0.00	0.00	0.00	0.00	20.78	0.39	0.00	0.00	0.00	99.07
Benstonite	12.51	5.73	2.03	0.13	0.16	0.00	24.39	1.08	0.98	0.00	20.69	4.33	0.00	27.17	0.00	0.00	0.59	0.00	99.79
Biotite	32.96	15.64	15.09	0.00	0.05	16.10	3.51	0.41	6.42	3.42	0.00	0.00	0.32	0.00	0.00	1.68	5.96	0.00	101.56
vermiculite1	30.92	8.17	23.56	0.00	0.00	10.15	6.60	4.95	4.14	2.88	0.00	0.00	0.00	0.00	0.00	0.00	7.54	1.09	100.00
vermiculite2	29.88	7.33	23.15	0.00	0.00	11.18	8.50	4.93	3.25	3.17	0.00	0.00	0.00	0.00	0.00	0.00	8.04	0.57	100.00
vermiculite3	32.45	24.47	4.09	0.00	0.00	9.96	11.20	1.27	4.08	2.19	0.00	0.00	0.00	0.00	0.00	0.00	7.97	1.61	99.29
vermiculite4	31.58	14.24	24.75	0.00	0.00	6.61	3.15	3.19	4.11	2.41	0.00	0.00	0.00	0.00	0.00	0.00	7.94	2.02	100.00
vermiculite5	31.64	10.47	21.36	0.00	0.00	12.26	3.15	2.39	5.05	3.17	0.00	0.00	0.00	0.00	0.00	0.00	8.18	2.33	100.00
vermiculite6	30.14	11.64	13.00	0.00	0.00	12.92	8.69	0.20	1.33	2.27	0.00	0.00	0.00	0.00	0.00	0.00	11.50	7.05	98.74
vermiculite7	22.44	13.99	3.42	0.00	0.00	9.02	23.97	2.39	0.88	1.22	0.00	0.00	0.00	0.00	0.00	0.00	19.93	2.82	100.08
vermiculite8	26.25	20.76	3.63	0.00	0.00	12.53	15.38	2.54	0.88	1.33	0.00	0.00	0.00	0.00	0.00	0.00	14.54	2.04	99.88
vermiculite9	26.41	20.48	3.76	0.00	0.00	8.24	20.46	2.27	0.82	1.61	0.00	0.00	0.00	0.00	0.00	0.00	13.72	1.88	99.65
vermiculite10	34.10	25.49	4.51	0.00	0.00	12.27	4.97	3.27	1.15	1.97	0.00	0.00	0.00	0.00	0.00	0.00	9.30	2.93	99.96
vermiculite11	21.82	13.70	3.68	0.00	0.00	7.39	24.93	1.41	0.60	0.99	0.00	0.00	0.00	0.00	0.00	0.00	22.01	3.83	100.36
vermiculite12	30.92	18.20	17.16	0.00	0.00	13.65	4.88	0.00	0.00	1.04	0.00	0.00	0.00	0.00	0.00	0.00	14.47	0.00	100.32
vermiculite13	32.15	21.58	12.51	0.00	0.23	4.36	4.89	0.18	1.52	3.01	0.00	0.00	0.00	0.00	0.00	0.00	18.12	0.00	98.55
Barite452	0.50	0.00	0.10	0.00	0.00	0.05	0.60	0.05	0.00	0.00	62.54	1.30	0.00	0.56	33.40	0.00	0.70	0.00	99.80
BariteAlan	4.56	0.17	0.06	0.00	0.00	0.00	1.00	0.00	0.00	0.00	58.74	4.54	0.00	0.05	30.66	0.00	0.08	0.00	99.86

Wo	wollastonite from wollastonite-calcite-garnet syenite								Epi	Epidote from skarn rock from Garigaipalli						Aps1, Aps2 and ap1			
apatite from Sevvattur carbonatites;					ap2,ap450		apatite from Onnakarai carbonatites						mt498	magnetitae from Sevvattur carbonatite					
Ice	Icelandspar from skarn rock of Garigaipalli							Cc250	Calcite from carbonaitte of Sevvattur						Cc310, cc311. cc312, cc313, cc314,				
Carbonates from carbonaites of Jogipatti						Cc492, cc493, cc494				carbonates from Carbonatites of Onnakarai							cc315		
Ben	Benstonite from Benstonite carbonatite from Onnakarai								Bi	Biotite from Biotite pyroxenite					verm 1-13		Vermiculite from		
Sevvattur carbonatites				Ba452	Barite from Onnakarai				BaAlan		Barite from Alangayam								

The chemical compositions of the rocks are listed in Tables 1 and 2 on the basis of rock types and their places of occurrence. The chemical compositions of these rocks vary widely in their silica, alkalis and carbonate contents. CO_2-rich rock carbonatites, Alkali syenites vary in SiO_2 between 35% and 65%, Ultramafic rocks vary in SiO_2 between 40% and 52%. Hybrid rocks have both SiO_2 and CO_2 in an intermediate position.

Table 2. Compositions of various minerals occurring in the carbonatite complex of Tiruppattur

Rock	No	Ba	Sr	Nb	Zr	La	Ce	Nd	Y	Th	U	V	Cu	Zn	Cr	Ni	Co	Pb	Sc
Sev sovite	Sub21		5225		5180	2690	2930	1900	45	140		450							
Sev beforsite	Sub22	3570	9700	220		350	1500	450	90	10	110								
Sev ferrocarbonaite	Sub23		4250	635	40	180	1860	570	130	30	40								
Jogi sovite	Sub24	35	300		10	25	40	10		10	10	10							
Gari skarn	Sub25	220	350		20	15	30			10	10	10							
Onna ferrocarbontite	Sub26	1159	7795	60	50	290	760	240	105	10	25	40							
Sev syenite	Sub11		270	740	120	200	650	430	200	50	10		20	20	15			120	
Sev syenite	Sub12	2780	1120	15	120	60		30	10				25	104	15			100	
Sev syenite	Sub13		955	35	260	70	120	45	30	15	10		20	50	25			170	
Sev ultramafic	Sub1		375		12	10	10	10	10			510							90
Jogi ultramafic	Sub2		275		15	10	25	10	10	10		40							55
Jogi ultramafic	Sub3		900		30	80	180	50	35										
Gari ultramafic	Sub4		217		20	10	10					90							40
Sev granite gneiss	Sub32	2321	1424	60	155	55			25	10	10		45	70	10			20	
Jogi syenite	Sub33	1726	900	60	170	55			30	30	10		20	50	20			35	
Jogi syenite	Sub34	1945	1120	35	240	60			20	15	10		20	60	15			180	
Jogi albitite	Sub35	220	30	180	350	20			10	250	100		10	15	35			10	
Jogi syenite	Sub36		470		80	10	25	50	50		10		20	20	10			880	
Jogi shonkinite	8	1000	2000		600				15			2000	1000	1000	1000	300	200	10	300
Jogi Riebeckite	R	600		60	30				10			200	9	100	2000	30	10	10	20
Jogi hy carbonatite	319	200	200		10				8			100	100	100	8	20	30		10
Jogi hy carbonatite	320	200			20							60	60	200	8	8	8		8
Jogi hy carbonatite	321	2000	2000		8				8			60	30			8	8	8	20
Jogi Rieb carbonatite	401	200	300	60	8				8			30	8	200	600	30	20	20	20
Jogi Rieb carbonatite	402	600	100		20							6010	8		100	30	30		10
Jogi Rieb carbonatite	490	100			10				8			10	8		30	10	10		
Jogi Wollastonite rock	491	300	300		8							60	300	100			8		
Jogi ultramafic nodule	497	2000			10							300	100	300	100	60	30		10
Jogi ultramafic	40	200	100		20				30			60	300	300	600	100	60	8	60
Sev ultramafic	201	3000	300	50	60				10			60	20	100		8	8	100	
Sev ultramafic	203	6000	2000	100	50				60			100	8	200	100	30	20	100	
Sev hy carbonatite	204		300		30				20			200	30	200	200	200	60		20
Sev hy carbonatite	206	600	600		60				60			100	100	100	600	100	60	20	60
Sev oligoclasite	219	1000	1000	60	100				10			300	60		30	10	10	20	
Jogi carbonatite	318	4000	1000	20	60				60			100	100	100	200	30	30	30	30
Apatite magnetite rock	460	100	100		8							200	300	100	300	30	30		8
Sev pyroxenite	789	300			400				10				100	60		60	60		60
Jogi ultramafic	493		790			170	145	90	950			50			100	175	75		675
Jogi ultrapot syenite	39	475	2300			880	380	790	2630			315	280	670	320	375	560	260	390
Jogi melanite sovite	990	120	4913		1115	250	165	123	733			78	73	110	73	73	160	133	610
Jogi shonkinite	561	322	5960		708	136	142	76	534			76	24	64	76	70	50	262	74

Table 3. Trace elements' distribution in carbonatites and associated alkaline rocks

10. Conclusion

The dolerites are hypabyssal equivalents of gabbro and basalts, which are common products of the partial melting of mantle / crustal rocks at depth. The overlapping petrographic

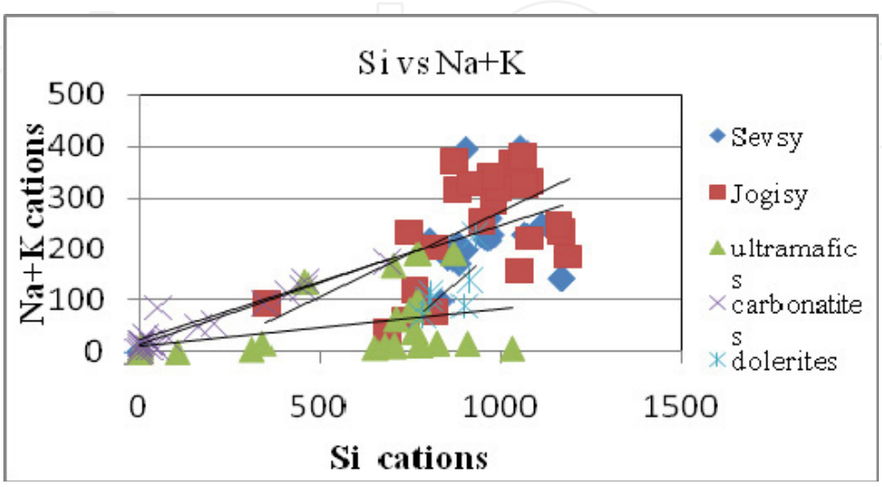

a)

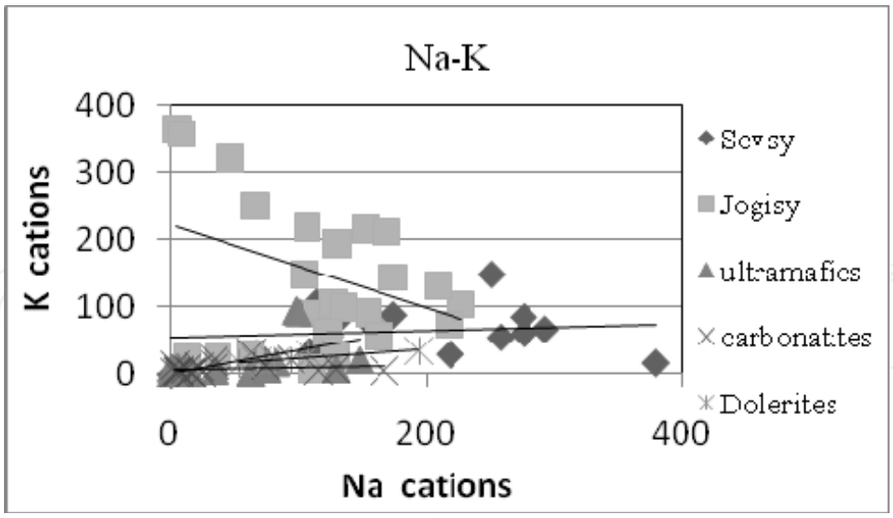
Na-K
400
300
200
100
0
K cations
0
200
400
Na cations
Sevsy
Jogisy
ultramafics
carbonatites
Dolerites

b)

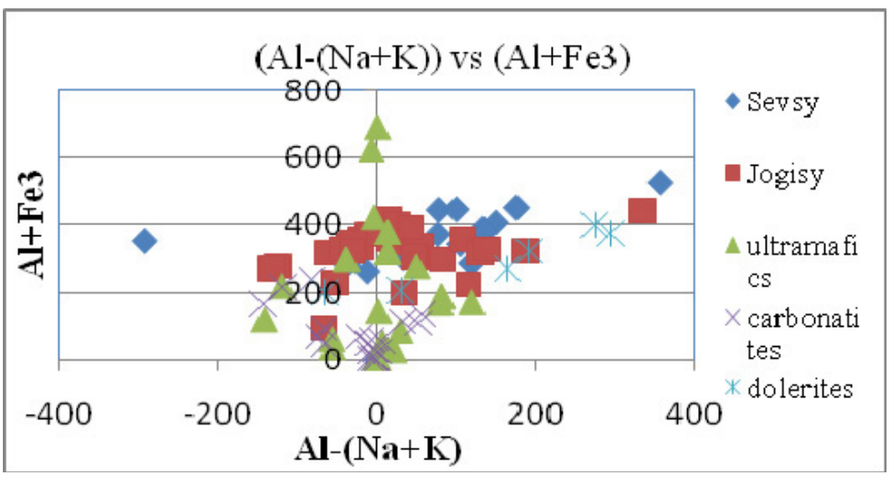
(Al-(Na+K)) vs (Al+Fe3)
800
600
400
200
0
Al+Fe3
-400
-200
0
200
400
Al-(Na+K)
Sevsy
Jogisy
ultramafi cs
carbonati tes
dolerites

c)

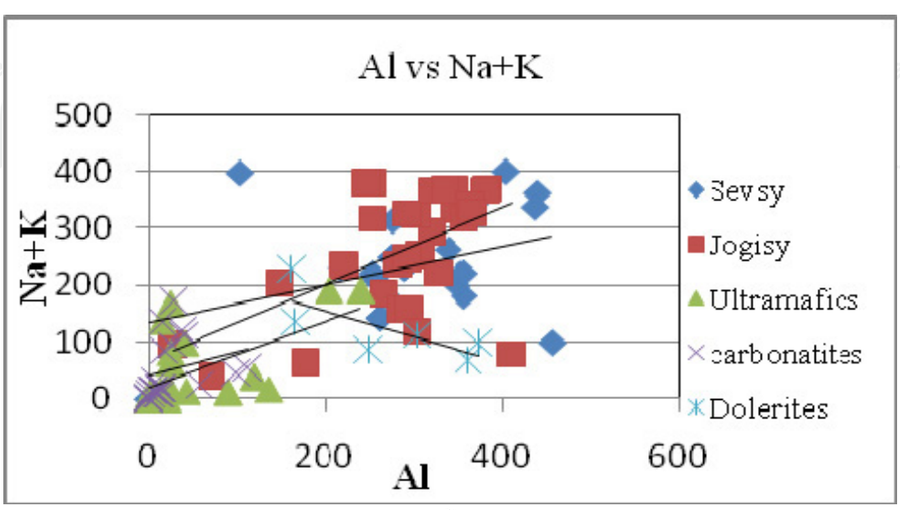
Al vs Na+K
500
400
300
200
100
0
Na+K
0
200
400
600
Al
Sevsy
Jogisy
Ultramafics
carbonatites
Dolerites

d)

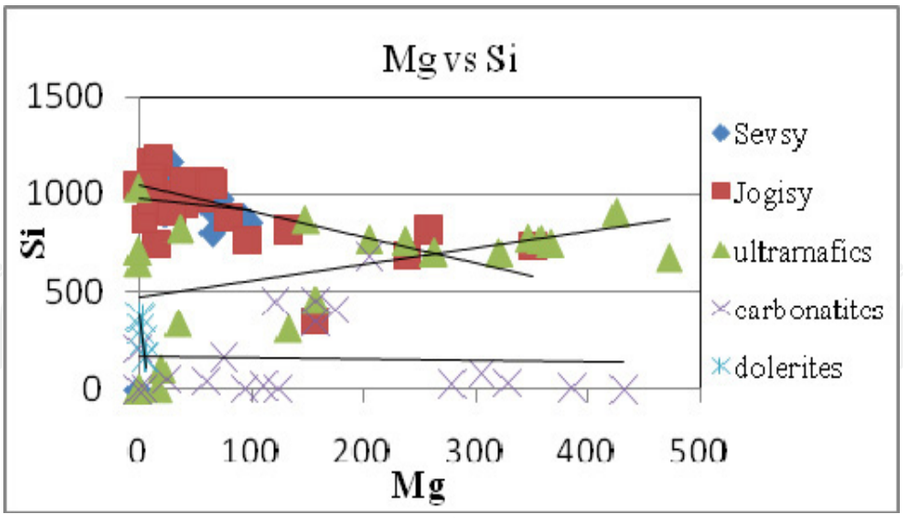
Mg vs Si
1500
1000
500
0
Si
0
100
200
300
400
500
Mg
Sevsy
Jogisy
ultramafics
carbonatites
dolerites

e)

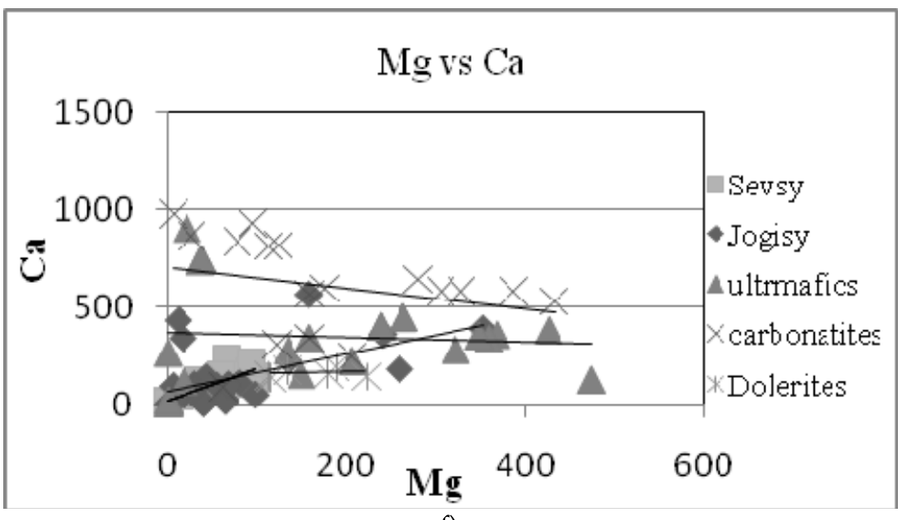
Mg vs Ca
1500
1000
500
0
Ca
0
200
400
600
Mg
Sevsy
Jogisy
ultrmafics
carbonatites
Dolerites

f)

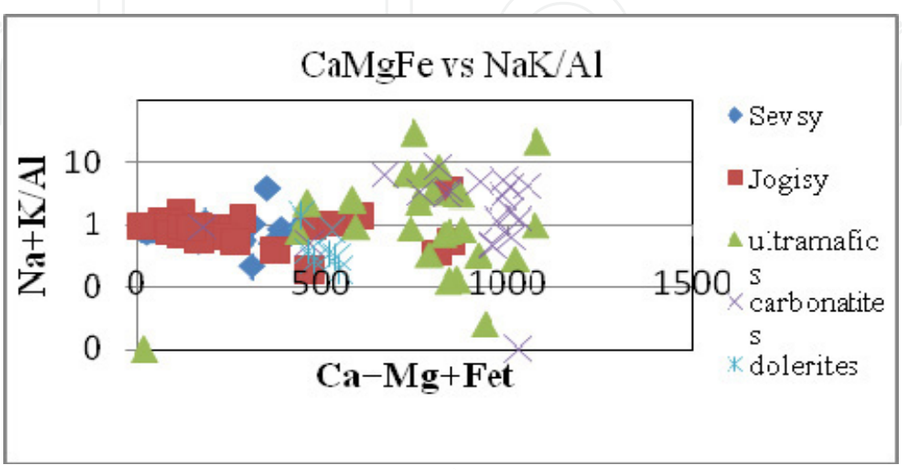
CaMgFe vs NaK/Al
10
1
0
0
Na+K/Al
0
500
1000
1500
Ca−Mg+Fet
Sevsy
Jogisy
ultramafics
carbonatites
dolerites

g)

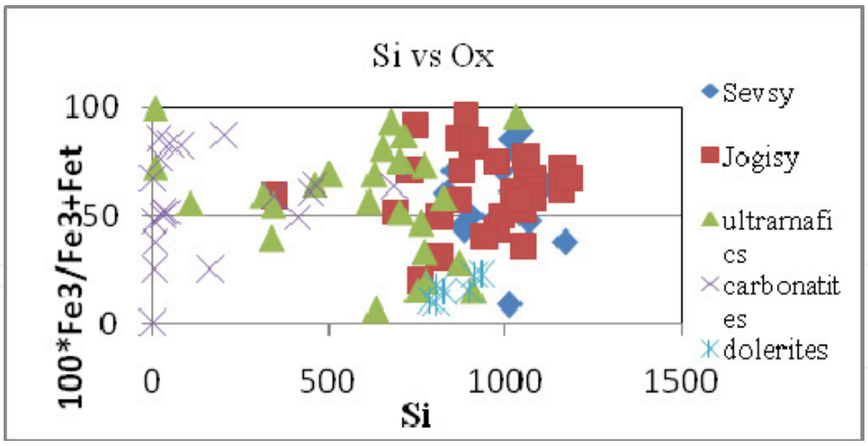

h)

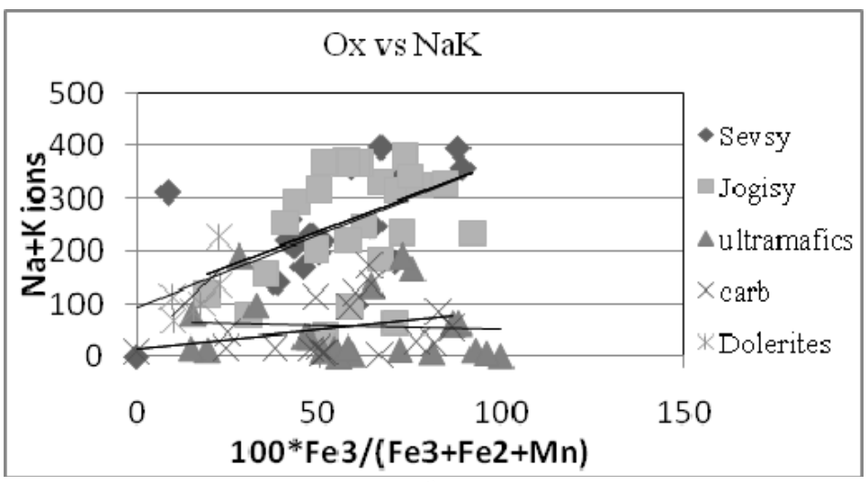

i)

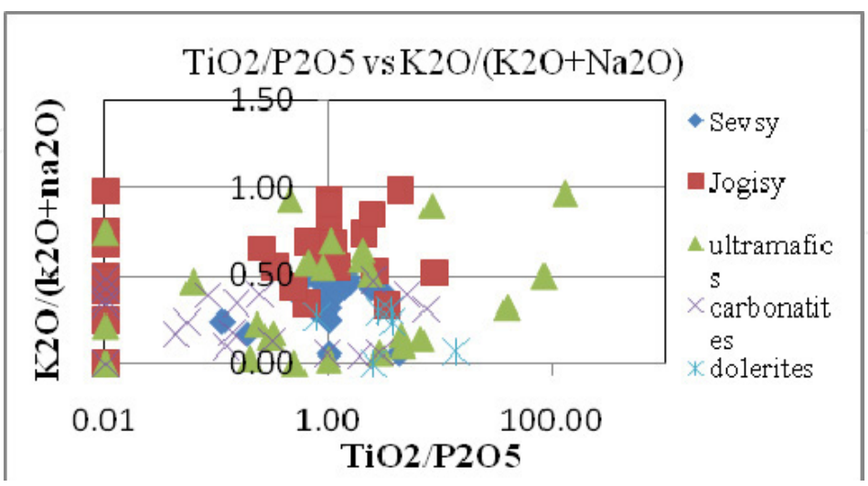

j)

Fig. 5. a-j show linear trends of the magmatic evolution of different types of rocks from common parent magma

variations of all these rocks indicate that they are all derived from the same mantle source by different degrees of partial melting. The composition of the parent magma for this complex appears to be very close in composition to that of shonkinite magma, which might have been derived by liquid fractionation and separation from the low degree of the partial melt of the mantle material. The partial melt might have initially been a crystallized olivine and calcic plagioclase; therefore, the residual shonkinitic parent magma so evolved is impoverished in alumina and in silica and acts as a primary magma in a closed magmatic chamber under volatile enriched conditions. Later on, with early crystallizations of calcium-rich clinopyroxenes, the residual magma is impoverished in silica with the enrichment of volatile constituents such as H_2O and CO_2. In an ascending convection current which motivated a low viscous and high temperature shonkinite magma, clinopyroxenes are crystallized with the enrichment of Ca, Mg, Fe, Ti^{iv} and Al^{iv} and a depletion in Si, Al^{vi}, Na and K in low pressure zones towards the top of the magmatic column. On the other hand, from the top of the magmatic column, sinking clinopyroxenes liberate Ca, Mg, Fe, Ti^{iv} and Al^{iv} and accumulate Na and Al^{vi} in their subsolidus crystal lattices during descending convection currents and towards the bottom of the chamber with the crystallization of subsolidus aegirine. Thus, both salic and mafic constituents in the form of ions are concentrated at the top of the magmatic column in different portions. In this closed magmatic chamber under high P_{H2O} and P_{CO2}, an immiscible separation of camafic carbonate liquids and alkali silicate liquids are derived at depth (Saravanan and Ramasamy, 1995). The separated alkali silicate magmas are emplaced in sequences of co-magmatic bodies of syenites, first in the Sevvattur Basin and subsequently emplaced in the Jogipatti basin followed by carbonate magmas in both (Fig. 1 a-d). It is quite a complex matter to study the impact of all these processes by tracing the history of the magmatic evolution inscribed on the rocks over the course of millions of years with the help of detailed petrographic and field investigations.

11. References

Barth, T.F.W. (1952) Theoretical Igneous Petrology, Ms Book and Mineral Company, 2nd Edn, New York, p. 416

Borodin, I.S., Gopal, V., Maralev, V.M. and Subramanian, V. (1971) Precambrian carbonatites of Tamil Nadu, South India, Journal of the Geological Society of India, v. 12, pp. 101-112

Bowen N.L. (1956) The Evolution of Igneous Rocks, Dover, New York, 2nd Edn, p. 332

Deer, W.A., Howie, R.A. and Zussman, J. (1965) Rock Forming Minerals, v. 1 to v. 5, Longmans, London

Dickson,J.A.D. (1965) A modified staining technique for carbonates in thin sections, Nature, v. 205, p. 587

Grady, J.C. (1971) Deep main faults in South India, Journal of the Geological Society of India, v. 12, pp. 56-62

von Eckermann, H. (1966) Wollastonite in carbonatite rocks, Geochimica et Cosmochimica Acta, v. 31 (11), pp. 2253-2254

Schieicher, H., Kramm, U., Pericka, E., Schidlowski, M., Schmidt, F., Subramanian, V., Todt, W. and Viladkar, S.G. (1998) Enriched sub-continental upper mantle beneath Southern India: Evidence from Pb, Nd, Sr and C-O Isotopic studies on Tamil Nadu carbonatites, Journal of Petrology, v. 39, (10)m, pp. 1765-85

Krishnan, M.S. (1962) Geology of India and Burma, Higgin Bothams, Chennai

Macintyre, R. (1975) Age and significance of carbonatites and alkaline intrusive, Mem. Noticicas. Mus. Lab. Min. Geol. Univ. Coimbra, v. 80, pp. 99-103

Mysen, B. (1975) Partitioning of iron and magnesium between crystals and partial melts in Peridotites Upper Mantle, Contrib, Mineral Petrol., v. 52, pp. 69-76

Mysen, B.O., Virgo, D. and Seifert, F.A. (1985) Relationships between properties and structure of aluminosilicate melts, Am. Mineralogist, v. 70, pp. 88-105

Naidu, P.R.J. (1958) 4-Axes Universal Stage, Dept. of Geology, Madras University

Ramasamy, R. (1973) Geology of the area South west of Tiruppattur, Madras State (Tamil Nadu), India, Ph.D Thesis, p. 226, University of Madras

Ramasamy, R. and Shapenko, V. (1980) Fluid inclusion studies in carbonatites of Tiruppattur, Tamil Nadu , India (Abst) Int. Geol. Cong. Paris , v. 1, p. 79

Ramasamy, R. (1981) Tectonomagmatic Episodes of the Peninsular India, Sympet, Jaipur, Geol. Surv. India, Abstract L2-L3.

Ramasamy, R. (1982a) A possible paleo-rift system of the eastern Ghats in the Peninsular India, J. Moscow State Univ., Geology, Ser. 4, No. 2, pp. 32-37 (in Russian)

Ramasamy, R. (1982) Structure and tectonics of carbonatite complex of Tiruppattur, Tamil Nadu In: Bhattacharya, A./K. (Ed.) Current Trends in Geology, IV Indian Geological Congress, Today and Tomorrows Publishers, New Delhi, pp. 119-136

Ramasamy, R. (1986) Titanium-bearing garnets from alkaline rocks of carbonatite complex of Tiruppattur, Tamil Nadu, Current Science, v. 55, pp. 1026-29

Ramasamy, R. (1986a) Ca-rich pyroxenes from the carbonatite complex of Tiruppattur, Tamil Nadu, Current Science, v. 55, pp. 981-984

Ramasamy, R. (1987) Reactivation of the Eastern Ghats Paleorift system during Tertiary and other periods, Proc. National, Seminar Tertiary Orogeny, pp. 109-127.

Ramasamy, R., Gwalani, L.G. and Subramanian, S.P. (2001) A note on the occurrence and formation of magnetite in the carbonatites of Sevvattur, North Arcot district, Tamil Nadu, Southern India Journal of Asian Earth Sciences, v. 19, pp. 297-304

Ramasamy, R., Subramanian, S.P. and Sundaravadivelu, R. (2010) Compositional variations of olivine in shonkinite and its associate ultrabasic rock from the carbonatite complex of Tiruppattur, Tamil Nadu, Current Science, v. 99(10), pp. 1428-1433

Rittmann, A. (1973) Stable Mineral Assemblage of Igneous Rocks, Springer, Berlin, p. 251

Saravanan, S. and Ramasamy, R. (1971) A magnesio-riebeckite from Samalpatti area, Tamil Nadu, India, Mineralogical Magazine, v. 38, pp. 376-377

Saravanan, S. and Ramasamy, R. (1995) Geochemistry and petrogenesis of shonkinite and associated alkaline rocks of Tiruppattur carbonatite complex, Tamil Nadu, Journal of the Geological Society of India, v. 46, pp. 235-243

Schairer, J.F. and Yoder, H.S.J.R., (1960) The nature of residual liquids from crystallization data on the system Nepheline-diopside-silica, American Journal of Science, Bradley Volume, v. 258A, pp. 273-83

Udas, G.R. and Krishnamurthy, P. (1970) Carbonatites of Sevvattur and Jogipatti, Madras State, India, Proc. Of the Indian National Academy of Science, 36A, pp. 331-343

Verwoerd, W.J. (1966) South African Carbonatites and their probable mode of origin, Ph.D. Thesis, Univ. of Stellenboch

Viladkar, S.G. and Subramanian, V. (1995) Mineralogy and geochemistry of the Sevvattur and Samalpatti complexes, Tamil Nadu, Journal of the Geological Society of India, v. 45, pp. 505-518

Winchell, A. N. (1945) Elements of Optical Mineralogy, part II Optical properties of Minerals

Yagi, K. (1953) Petrochemical studies on the alkaline rocks of the Morotu District, Sakhalin, GSA Bull, v. 64, 769-810

Yoder, H.S., Stewart, D.B. and Smith, J.R. (1957) Ternary feldspars, Carnegie Inst. Washington Year Book, pp. 206-214